

MULTI-ANTENNA INFORMATION THEORY

W. Geyi

Research In Motion
185 Columbia St. W., Waterloo, Ontario, Canada N2L 5Z5

Abstract—It is well known that the performance of a wireless multiple-input and multiple-output (MIMO) system depends on the propagation channel. The propagation channel models can generally be divided into two different groups, the statistical models based on information theory and the site-specific models based on measurement or ray tracing. In this paper, a general procedure for predicting the MIMO channel model has been presented. Analytical expressions for the channel matrix elements in a general scattering environment have been derived from the statistical theory for a narrow-band electromagnetic field, and have been verified by numerical simulation and experiments. The limitations of information capacity of the MIMO wireless communication system imposed by the antennas have also been discussed, and analytical upper bounds on the information capacity in terms of the antenna parameters for multiple antenna system in free space have been obtained. Once the capacity of a MIMO system is specified, these upper bounds can serve as a criterion for estimating how many antennas are needed or how big the antenna must be to achieve the capacity.

1. INTRODUCTION

An important performance index for characterizing a communication system is the spectral efficiency measured in bit/s/Hz. Shannon's channel capacity theorem reveals that there is a maximum spectral efficiency, called channel capacity, at which any communication system can operate reliably [1, 2]. The multiple-input multiple-output (MIMO) system has emerged as one of the most promising technologies to increase the capacity of the wireless link [3–6]. In a MIMO wireless system, multiple antenna elements are deployed and the data stream from a single user is demultiplexed into n_t (the number of transmitting antennas) substreams. Each substream is then encoded into channel

symbols, and the signals are received by n_r receiving antennas. Various coding schemes, such as layered space-time codes, space-time Trellis codes and space-time block codes, have been proposed to exploit the benefits of MIMO channels.

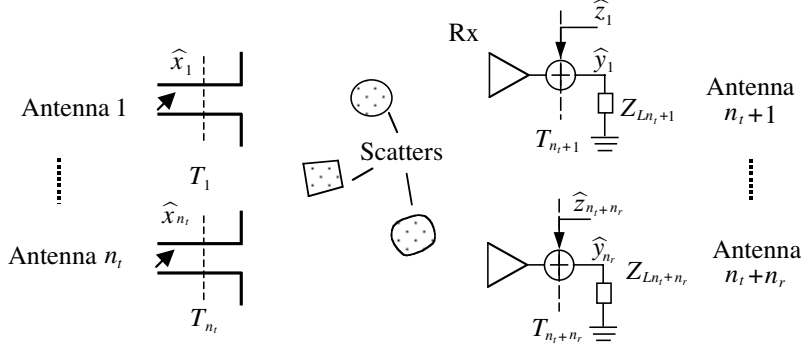


Figure 1. An arbitrary MIMO system.

A general linear time-invariant MIMO system with n_t inputs and n_r outputs is shown in Figure 1, where T_i ($i = 1, 2, \dots, n_t + n_r$) is the i th antenna terminal plane (i.e., the reference plane), and the n_r outputs are terminated by loads Z_{L_i} at T_i ($i = n_t + 1, \dots, n_t + n_r$). The output random signal vector $\mathbf{y}(t) = [y_{n_t+1}(t), y_{n_t+2}(t), \dots, y_{n_t+n_r}(t)]^T \in R^{n_r}$ (R^{n_r} is the n dimensional real space) is related to the input random signal vector $\mathbf{x}(t) = [x_1(t), x_2(t), \dots, x_{n_t}(t)]^T \in R^{n_t}$ by the following convolution integral [3]

$$\mathbf{y}(t) = \int_{-\infty}^{\infty} \mathbf{h}(\tau) \mathbf{x}(t - \tau) d\tau + \mathbf{z}(t) \quad (1)$$

where $\mathbf{z}(t) = [z_{n_t+1}(t), z_{n_t+2}(t), \dots, z_{n_t+n_r}(t)]^T \in R^{n_r}$ is assumed to be the zero-mean additive white Gaussian noise (AWGN) vector whose components have a power spectral density σ^2 , and $\mathbf{h}(t) = \{h_{ij}(t)\}$ is the impulse response matrix (or channel matrix) of the MIMO system with $h_{ij}(t)$ being the impulse response between the j th ($j = 1, 2, \dots, n_t$) transmitting antenna and the i th receiving antenna ($i = n_t + 1, n_t + 2, \dots, n_t + n_r$). In most applications, communications are carried out in a passband around a carrier frequency ω_c . Thus one may write [7, 8]

$$\mathbf{x}(t) = \text{Re} [\hat{\mathbf{x}}(t)e^{j\omega_c t}], \quad \mathbf{y}(t) = \text{Re} [\hat{\mathbf{y}}(t)e^{j\omega_c t}], \quad \mathbf{z}(t) = \text{Re} [\hat{\mathbf{z}}(t)e^{j\omega_c t}]$$

where $\hat{\mathbf{x}}(t)$, $\hat{\mathbf{y}}(t)$ and $\hat{\mathbf{z}}(t)$ are the complex envelopes of $\mathbf{x}(t)$, $\mathbf{y}(t)$ and $\mathbf{z}(t)$ respectively (a caret ‘ $\hat{\cdot}$ ’ will be used to represent the complex envelope), and they all belong to the n -dimensional complex space C^n . As usual, if the bandwidth of the input signal vector is narrow the Fourier transform of $\mathbf{h}(t)$ will be treated as a constant over the band of interest. Then (1) can be approximated by [3]

$$\hat{\mathbf{y}}(t) \approx \underline{\mathbf{H}}\hat{\mathbf{x}}(t) + \hat{\mathbf{z}}(t) \quad (2)$$

where $\underline{\mathbf{H}} = \mathbf{h}(0)$. For the simulation and design of a MIMO system, precise knowledge about the channel matrix $\underline{\mathbf{H}}$ is needed. Numerous MIMO channel models have been proposed to characterize the complicated propagation environments [9–14], such as statistical models and site-specific models based on ray tracing. The usual statistical channel models include the Rayleigh fading channel model for non-line-of-sight scenarios and the Rician fading channel model for line-of-sight scenarios. A shortcoming of these statistical descriptions for a wireless MIMO channel is that they do not explicitly contain the information about the physical parameters, such as antenna gain. In addition, these statistical descriptions depend on the measuring equipments, and the influences of the channel and equipments on the channel model cannot be separated [15]. Therefore the channel models that include physical parameters are preferred.

It has been noted that incorporating electromagnetics into the methodologies of signal processing and communication theory will lead to a better solution when deploying a system in a real environment [16]. In this paper, a general procedure of predicting the MIMO channel model from an electromagnetic point of view has been presented, which is based on the scattering matrix description of the MIMO system. The channel model so obtained has included all the physical parameters such as the influences of antennas, from which a connection can be established between the system capacity and antenna parameters. When the upper bounds of the antenna performances [17–19] are taken into account in this connection, the upper bound of information capacity of a wireless MIMO system can then be determined. The paper is organized as follows. Section 2 discusses briefly the narrow-band stationary stochastic process for electromagnetic field, and it is demonstrated that the conventional time-harmonic theory of electromagnetic field also holds for the complex envelopes as well as the ensemble average of the complex envelopes of a narrow-band stationary electromagnetic field. Section 3 studies the capacity of a general deterministic MIMO system and it is shown that the channel matrix can be identified as the scattering matrix, and upper bounds on the system capacity have been obtained in terms of the scattering

parameters. Section 4 provides a general procedure to calculate the channel matrix in free space as well as in a scattering environment, which has been verified by numerical simulation and experiments. Section 5 summarizes the upper bounds on the antenna performances and discusses upper bounds of capacity for various MIMO system in free space and explains how the upper bounds of information capacity can be applied to estimate the antenna numbers and antenna sizes required to achieve the capacity requirement, which answers a frequently asked question of whether there is a fundamental limit as to how many independent antennas can be squeezed into a given small volume to satisfy a given capacity requirement [20].

2. NARROW-BAND STATIONARY STOCHASTIC VECTOR FIELD

As a linear modulation technique, an easy way to translate the spectrum of low-pass or baseband signal $a(t)$ to a higher frequency is to multiply or heterodyne the baseband signal with a carrier wave. A narrowband bandpass stochastic vector field \mathbf{F} (modulated signal) in the time domain can be expressed as [7, 8]

$$\mathbf{F}(\mathbf{r}, t) = \begin{cases} \mathbf{a}(\mathbf{r}, t) \cos[\omega_c t + \varphi(\mathbf{r}, t)] \\ \mathbf{x}(\mathbf{r}, t) \cos \omega_c t - \mathbf{y}(\mathbf{r}, t) \sin \omega_c t \\ \text{Re } \widehat{\mathbf{F}}(\mathbf{r}, t) e^{j\omega_c t} \end{cases}$$

where $\omega_c = 2\pi f_c$, $\mathbf{a}(\mathbf{r}, t)$ and $\varphi(\mathbf{r}, t)$ are the carrier frequency, envelope and phase of the modulated signal respectively, and

$$\begin{aligned} \widehat{\mathbf{F}}(\mathbf{r}, t) &= \mathbf{x}(\mathbf{r}, t) + j\mathbf{y}(\mathbf{r}, t) \\ \mathbf{x}(\mathbf{r}, t) &= \mathbf{a}(\mathbf{r}, t) \cos \varphi(\mathbf{r}, t) \\ \mathbf{y}(\mathbf{r}, t) &= \mathbf{a}(\mathbf{r}, t) \sin \varphi(\mathbf{r}, t) \end{aligned}$$

in which $\widehat{\mathbf{F}}(\mathbf{r}, t)$, $\mathbf{x}(\mathbf{r}, t)$ and $\mathbf{y}(\mathbf{r}, t)$ are the complex envelope, in-phase component, and quadrature component of the modulated signal respectively. The complex envelope $\widehat{\mathbf{F}}(\mathbf{r}, t)$ is slowly varying function of time compared to $e^{j\omega_c t}$. It is easy to show that the complex envelopes of the electromagnetic fields satisfy the time-harmonic Maxwell equations

$$\begin{cases} \nabla \times \widehat{\mathbf{H}}(\mathbf{r}, t) = j\omega_c \varepsilon \widehat{\mathbf{E}}(\mathbf{r}, t) + \widehat{\mathbf{J}}(\mathbf{r}, t) \\ \nabla \times \widehat{\mathbf{E}}(\mathbf{r}, t) = -j\omega_c \mu \widehat{\mathbf{H}}(\mathbf{r}, t) \end{cases} \quad (3)$$

where all notations have their conventional meaning. Therefore most of the theoretical results about the time-harmonic fields can be applied to

the complex envelopes of the fields. Let $\overline{\mathbf{F}}$ denote the ensemble average of \mathbf{F} . For a stationary and ergodic vector field \mathbf{F} , the ensemble average equals the time average, i.e., $\overline{\mathbf{F}} = \lim_{T \rightarrow \infty} \frac{1}{T} \int_{-T/2}^{T/2} \mathbf{F}(t) dt$. For a stationary and ergodic electromagnetic field, one may take the ensemble average of (3) to get

$$\begin{cases} \nabla \times \overline{\widehat{\mathbf{H}}(\mathbf{r})} = j\omega_c \varepsilon \overline{\widehat{\mathbf{E}}(\mathbf{r})} + \overline{\widehat{\mathbf{J}}(\mathbf{r})} \\ \nabla \times \overline{\widehat{\mathbf{E}}(\mathbf{r})} = -j\omega_c \mu \overline{\widehat{\mathbf{H}}(\mathbf{r})} \end{cases} \quad (4)$$

Hence most of the theoretical results about the time-harmonic fields can also be applied to the ensemble averages of the complex envelopes of the fields. The autocorrelation function $R_{\mathbf{F}\mathbf{F}}(\tau)$ of a vector field \mathbf{F} can be expressed as

$$R_{\mathbf{F}\mathbf{F}}(\tau) = \overline{\mathbf{F}(t+\tau) \cdot \widehat{\mathbf{F}}(t)} = \frac{1}{2} \text{Re} [R_{\widehat{\mathbf{F}}\widehat{\mathbf{F}}}(\tau) e^{j\omega_c \tau}]$$

where $\widehat{\mathbf{F}}$ denotes the complex conjugate of \mathbf{F} . From now on, all the electromagnetic fields will be assumed to be a narrow-band stochastic process and the time dependence in the complex envelope notations will be dropped.

3. CAPACITY OF DETERMINISTIC MIMO SYSTEM

The MIMO system capacity is defined as the maximum mutual information over all possible input vector signals [21–24]. The mutual information between $\widehat{\mathbf{x}}$ and $\widehat{\mathbf{y}}$ is denoted by $I(\widehat{\mathbf{x}}, \widehat{\mathbf{y}})$. The capacity (measured in bit/s/Hz) of a deterministic MIMO system is then given by [3–6]

$$\begin{aligned} C &= \sup_{\text{Tr}(\mathbf{R}_{\widehat{\mathbf{x}}\widehat{\mathbf{x}}})=P} I(\widehat{\mathbf{x}}, \widehat{\mathbf{y}}) \\ &= \sup_{\text{Tr}(\mathbf{R}_{\widehat{\mathbf{x}}\widehat{\mathbf{x}}})=P} \log_2 \det \left[\mathbf{I}_{n_r} + \underline{\mathbf{H}} \mathbf{R}_{\widehat{\mathbf{x}}\widehat{\mathbf{x}}} \underline{\mathbf{H}}^\dagger (\mathbf{R}_{\widehat{\mathbf{z}}\widehat{\mathbf{z}}})^{-1} \right] \end{aligned} \quad (5)$$

where $\mathbf{R}_{\mathbf{k}\mathbf{k}}$ is the covariance matrix for the vector \mathbf{k} ($\mathbf{k} = \widehat{\mathbf{x}}, \widehat{\mathbf{z}}$); \mathbf{I}_n is an $n \times n$ identity matrix; and P is the total transmitted power, which is kept constant regardless of the number of transmitting antennas. It is common to assume that the noises in the receiver branches are uncorrelated so that one can write $\mathbf{R}_{\widehat{\mathbf{z}}\widehat{\mathbf{z}}} = \sigma^2 \mathbf{I}_{n_r}$. Thus (5) may be

written as

$$\begin{aligned} C &= \sup_{\text{Tr}(\mathbf{R}_{\hat{\mathbf{x}}\hat{\mathbf{x}}})=P} \log_2 \det \left(\mathbf{I}_{n_r} + \frac{1}{\sigma^2} \mathbf{H} \mathbf{R}_{\hat{\mathbf{x}}\hat{\mathbf{x}}} \mathbf{H}^\dagger \right) \\ &= \sup_{\text{Tr}(\mathbf{R}_{\hat{\mathbf{x}}\hat{\mathbf{x}}})=P} \log_2 \det \left(\mathbf{I}_{n_t} + \frac{1}{\sigma^2} \mathbf{R}_{\hat{\mathbf{x}}\hat{\mathbf{x}}} \mathbf{H}^\dagger \mathbf{H} \right) \end{aligned} \quad (6)$$

where the determinant identity $\det(I + AB) = \det(I + BA)$ has been used. In practice the input has no knowledge about the channel matrix \mathbf{H} . For this reason one can choose $\hat{\mathbf{x}}$ to be spatially white (i.e., signals on each input port are independent) and use a uniform power distribution (i.e., each input is equi-powered). In this case the covariance matrix of $\hat{\mathbf{x}}$ is given by $\mathbf{R}_{\hat{\mathbf{x}}\hat{\mathbf{x}}} = (P/n_t)\mathbf{I}_{n_t}$, and (6) reduces to

$$C = \log_2 \det \left(\mathbf{I}_{n_r} + \frac{P}{\sigma^2 n_t} \mathbf{H} \mathbf{H}^\dagger \right) = \log_2 \det \left(\mathbf{I}_{n_t} + \frac{P}{\sigma^2 n_t} \mathbf{H}^\dagger \mathbf{H} \right) \quad (7)$$

Once the channel matrix is known the capacity is then determined. For the $n_t \times n_r$ MIMO system shown in Figure 1, the modal voltage \widehat{V}_i and modal current \widehat{I}_i at a reference plane T_i for the antenna element i are defined by $\widehat{\mathbf{E}}(\mathbf{r}) = \widehat{V}_i \mathbf{e}_i$, $\widehat{\mathbf{H}}(\mathbf{r}) = \widehat{I}_i \mathbf{u}_n \times \mathbf{e}_i$ [25], where $\widehat{\mathbf{E}}$ and $\widehat{\mathbf{H}}$ are the complex envelopes of the transverse fields inside the feeding line; \mathbf{e}_i denotes the dominant vector mode function of the feeding line for the i th antenna element; and \mathbf{u}_n is the unit vector perpendicular to the reference plane T_i , as shown in Figure 2. Let the normalized incident and reflected waves at the antenna terminal T_i be denoted by \widehat{a}_i and \widehat{b}_i respectively. By definition, one may write

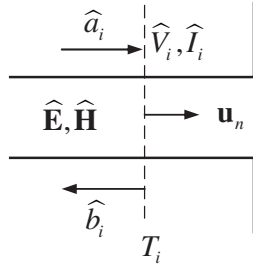


Figure 2. An arbitrary antenna.

$$\begin{cases} \widehat{V}_i = \frac{\overline{Z}_{si}}{\sqrt{\text{Re } Z_{si}}} \widehat{a}_i + \frac{Z_{si}}{\sqrt{\text{Re } Z_{si}}} \widehat{b}_i \\ \widehat{I}_i = \frac{1}{\sqrt{\text{Re } Z_{si}}} \widehat{a}_i - \frac{1}{\sqrt{\text{Re } Z_{si}}} \widehat{b}_i \end{cases}, \quad i = 1, 2, \dots, n_t + n_r \quad (8)$$

where Z_{si} is the reference impedance for the input terminal of antenna element i . For a noisy MIMO network, the relationship between the normalized incident wave and reflected wave can be expressed as [26]

$$\begin{bmatrix} \widehat{b}_1 \\ \vdots \\ \widehat{b}_{n_t} \\ \widehat{b}_{n_t+1} \\ \vdots \\ \widehat{b}_{n_t+n_r} \end{bmatrix} = \begin{bmatrix} S_{11} & \cdots & S_{1n_t} & S_{1(n_t+1)} & \cdots & S_{1(n_t+n_r)} \\ \vdots & \ddots & \vdots & \vdots & \ddots & \vdots \\ S_{n_t1} & \cdots & S_{n_t n_t} & S_{n_t(n_t+1)} & \cdots & S_{n_t(n_t+n_r)} \\ S_{(n_t+1)1} & \cdots & S_{(n_t+1)n_t} & S_{(n_t+1)(n_t+1)} & \cdots & S_{(n_t+1)(n_t+n_r)} \\ \vdots & \ddots & \vdots & \vdots & \ddots & \vdots \\ S_{(n_t+n_r)1} & \cdots & S_{(n_t+n_r)n_t} & S_{(n_t+n_r)(n_t+1)} & \cdots & S_{(n_t+n_r)(n_t+n_r)} \end{bmatrix} \times \begin{bmatrix} \widehat{a}_1 \\ \vdots \\ \widehat{a}_{n_t} \\ \widehat{a}_{n_t+1} \\ \vdots \\ \widehat{a}_{n_t+n_r} \end{bmatrix} + \begin{bmatrix} \widehat{b}_1^n \\ \vdots \\ \widehat{b}_{n_t}^n \\ \widehat{b}_{n_t+1}^n \\ \vdots \\ \widehat{b}_{n_t+n_r}^n \end{bmatrix} \quad (9)$$

where S_{ij} is the transmission coefficient from antenna j to antenna i , and \widehat{b}_i^n is the normalized noise wave which will be assumed to be a zero-mean white Gaussian noise. Taking the ensemble average of (9) and making use of the assumption that the channel is deterministic and \widehat{b}_i^n ($i = 1, 2, \dots, n_t + n_r$) have zero mean lead to

$$\begin{aligned}
& \begin{bmatrix} \overline{\widehat{b}}_1 \\ \vdots \\ \overline{\widehat{b}}_{n_t} \\ \overline{\widehat{b}}_{n_t+1} \\ \vdots \\ \overline{\widehat{b}}_{n_t+n_r} \end{bmatrix} = \\
& \begin{bmatrix} S_{11} & \cdots & S_{1n_t} & S_{1(n_t+1)} & \cdots & S_{1(n_t+n_r)} \\ \vdots & \ddots & \vdots & \vdots & \ddots & \vdots \\ S_{n_t 1} & \cdots & S_{n_t n_t} & S_{n_t(n_t+1)} & \cdots & S_{n_t(n_t+n_r)} \\ S_{(n_t+1)1} & \cdots & S_{(n_t+1)n_t} & S_{(n_t+1)(n_t+1)} & \cdots & S_{(n_t+1)(n_t+n_r)} \\ \vdots & \ddots & \vdots & \vdots & \ddots & \vdots \\ S_{(n_t+n_r)1} & \cdots & S_{(n_t+n_r)n_t} & S_{(n_t+n_r)(n_t+1)} & \cdots & S_{(n_t+n_r)(n_t+n_r)} \end{bmatrix} \\
& \times \begin{bmatrix} \overline{\widehat{a}}_1 \\ \vdots \\ \overline{\widehat{a}}_{n_t} \\ \overline{\widehat{a}}_{n_t+1} \\ \vdots \\ \overline{\widehat{a}}_{n_t+n_r} \end{bmatrix} \tag{10}
\end{aligned}$$

Hereafter all antennas will be assumed to be matched so that $\overline{\widehat{b}}_1 = \cdots = \overline{\widehat{b}}_{n_t} = 0$ and $\overline{\widehat{a}}_{n_t+1} = \cdots = \overline{\widehat{a}}_{n_t+n_r} = 0$. Then (10) reduces to

$$\begin{bmatrix} \overline{\widehat{b}}_{n_t+1} \\ \vdots \\ \overline{\widehat{b}}_{n_t+n_r} \end{bmatrix} = \begin{bmatrix} S_{(n_t+1)1} & \cdots & S_{(n_t+1)n_t} \\ \vdots & \ddots & \vdots \\ S_{(n_t+n_r)1} & \cdots & S_{(n_t+n_r)n_t} \end{bmatrix} \begin{bmatrix} \overline{\widehat{a}}_1 \\ \vdots \\ \overline{\widehat{a}}_{n_t} \end{bmatrix} \tag{11}$$

Comparing (11) with the ensemble average of (2), the following identifications can be made

$$\begin{aligned}
 \underline{\mathbf{H}} &= \begin{bmatrix} S_{(n_t+1)1} & \cdots & S_{(n_t+1)n_t} \\ \vdots & \ddots & \vdots \\ S_{(n_t+n_r)1} & \cdots & S_{(n_t+n_r)n_t} \end{bmatrix} \\
 \overline{\underline{\mathbf{x}}} &= \left[\overline{\overline{a_1}}/\sqrt{2}, \overline{\overline{a_2}}/\sqrt{2}, \dots, \overline{\overline{a_{n_t}}}/\sqrt{2} \right]^T \\
 \overline{\underline{\mathbf{y}}} &= \left[\overline{\overline{b_{n_t+1}}}/\sqrt{2}, \overline{\overline{b_{n_t+2}}}/\sqrt{2}, \dots, \overline{\overline{b_{n_t+n_r}}}/\sqrt{2} \right]^T
 \end{aligned} \tag{12}$$

Substituting (12) into (7) gives

$$C = \log_2 \det \left(\mathbf{I}_{n_t} + \frac{P}{\sigma^2 n_t} \begin{bmatrix} \sum_{i=1}^{n_r} |S_{(n_t+i)1}|^2 & \sum_{i=1}^{n_r} \overline{S}_{(n_t+i)1} S_{(n_t+i)2} & \cdots & \sum_{i=1}^{n_r} \overline{S}_{(n_t+i)1} S_{(n_t+i)n_t} \\ \sum_{i=1}^{n_r} \overline{S}_{(n_t+i)2} S_{(n_t+i)1} & \sum_{i=1}^{n_r} |S_{(n_t+i)2}|^2 & \cdots & \sum_{i=1}^{n_r} \overline{S}_{(n_t+i)2} S_{(n_t+i)n_t} \\ \vdots & \vdots & \ddots & \vdots \\ \sum_{i=1}^{n_r} \overline{S}_{(n_t+i)n_t} S_{(n_t+i)1} & \sum_{i=1}^{n_r} \overline{S}_{(n_t+i)n_t} S_{(n_t+i)2} & \cdots & \sum_{i=1}^{n_r} |S_{(n_t+i)n_t}|^2 \end{bmatrix} \right) \tag{13}$$

$$C = \log_2 \det \left(\mathbf{I}_{n_r} + \frac{P}{\sigma^2 n_t} \right)$$

$$\left[\begin{array}{cccc} \sum_{i=1}^{n_t} |S_{(n_t+1)i}|^2 & \sum_{i=1}^{n_t} S_{(n_t+1)i} \bar{S}_{(n_t+2)i} & \cdots & \sum_{i=1}^{n_t} S_{(n_t+1)i} \bar{S}_{(n_t+n_r)i} \\ \sum_{i=1}^{n_t} S_{(n_t+2)i} \bar{S}_{(n_t+1)i} & \sum_{i=1}^{n_t} |S_{(n_t+2)i}|^2 & \cdots & \sum_{i=1}^{n_t} S_{(n_t+2)i} \bar{S}_{(n_t+n_r)i} \\ \vdots & \vdots & \ddots & \vdots \\ \sum_{i=1}^{n_t} S_{(n_t+n_r)i} \bar{S}_{(n_t+1)i} & \sum_{i=1}^{n_t} S_{(n_t+n_r)i} \bar{S}_{(n_t+2)i} & \cdots & \sum_{i=1}^{n_t} |S_{(n_t+n_r)i}|^2 \end{array} \right] \quad (14)$$

Since $\underline{\mathbf{H}}^\dagger \underline{\mathbf{H}}$ and $\underline{\mathbf{H}} \underline{\mathbf{H}}^\dagger$ are positive definite, it follows from Hadamard's inequality [27, 28] that

$$C \leq \log_2 \prod_{j=1}^{n_t} \left(1 + \frac{P}{\sigma^2 n_t} \sum_{i=1}^{n_r} |S_{(n_t+i)j}|^2 \right) = \sum_{j=1}^{n_t} \log_2 \left(1 + \frac{P}{\sigma^2 n_t} \sum_{i=1}^{n_r} |S_{(n_t+i)j}|^2 \right) \quad (15)$$

$$C \leq \log_2 \prod_{j=1}^{n_r} \left(1 + \frac{P}{\sigma^2 n_t} \sum_{i=1}^{n_t} |S_{(n_t+j)i}|^2 \right) = \sum_{j=1}^{n_r} \log_2 \left(1 + \frac{P}{\sigma^2 n_t} \sum_{i=1}^{n_t} |S_{(n_t+j)i}|^2 \right) \quad (16)$$

The right-hand sides of (15) and (16) are upper bounds on the information capacity of the MIMO system.

4. CALCULATION OF CHANNEL MATRIX

The elements of the channel matrix can be determined from electromagnetic theory. Consider a system consisting of n antennas contained in a region V_∞ bounded by S_∞ . Let the fields generated by antenna i ($i = 1, 2, \dots, n$) when antenna j ($j \neq i$) are receiving with all scatters being in place be denoted by $\overline{\mathbf{E}}_i, \overline{\mathbf{H}}_i$ (ensemble averages), and V_i be the source region of antenna i , which is chosen in such a way that its boundary, denoted by S_i , is coincident with the metal surface of the antennas except for a portion of the reference plane T_i . This state of operation is illustrated in Figure 3, where the medium around the antenna is assumed to be isotropic and inhomogeneous. To calculate the scattering parameter S_{ij} , the frequency-domain reciprocity theorem for the ensemble averages of the complex envelopes

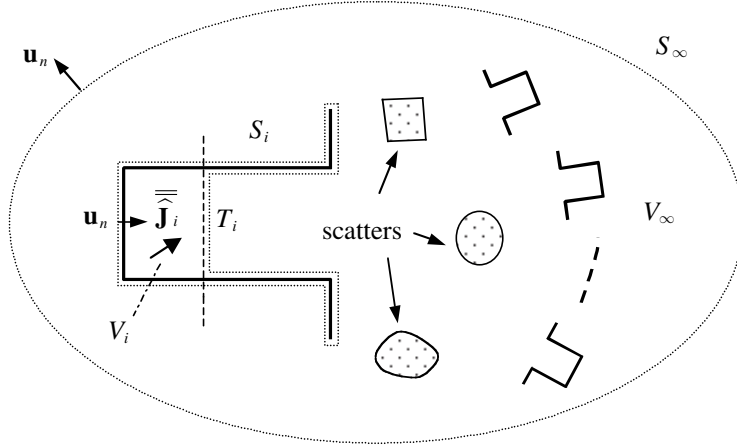


Figure 3. Derivation of scattering parameters.

may be used [29]

$$\int_S \left(\overline{\overline{\mathbf{E}}_i} \times \overline{\overline{\mathbf{H}}_j} - \overline{\overline{\mathbf{E}}_j} \times \overline{\overline{\mathbf{H}}_i} \right) \cdot \mathbf{u}_n ds = 0 \quad (17)$$

where it is assumed that the closed surface S does not contain any impressed sources. The closed surface S can be chosen as $S_\infty + \sum_{l=1}^n S_l$ in (17) so that

$$\begin{aligned} & \sum_{l=1}^n \int_{S_l} \left(\overline{\overline{\mathbf{E}}_i} \times \overline{\overline{\mathbf{H}}_j} - \overline{\overline{\mathbf{E}}_j} \times \overline{\overline{\mathbf{H}}_i} \right) \cdot \mathbf{u}_n ds + \int_{S_\infty} \left(\overline{\overline{\mathbf{E}}_i} \times \overline{\overline{\mathbf{H}}_j} - \overline{\overline{\mathbf{E}}_j} \times \overline{\overline{\mathbf{H}}_i} \right) \cdot \mathbf{u}_n ds \\ &= \sum_{l=1}^n \left(\overline{\overline{\widehat{V}}_l^{(j)}} \overline{\overline{\widehat{I}}_l^{(i)}} - \overline{\overline{\widehat{V}}_l^{(i)}} \overline{\overline{\widehat{I}}_l^{(j)}} \right) = 0 \end{aligned} \quad (18)$$

Here the feeding lines have been assumed to be in a single mode operation so that the following calculation applies

$$\int_{S_l} \left(\overline{\overline{\mathbf{E}}_i} \times \overline{\overline{\mathbf{H}}_i} \right) \cdot \mathbf{u}_n ds = -\overline{\overline{\widehat{V}}_l^{(i)}} \overline{\overline{\widehat{I}}_l^{(i)}}, \quad l = 1, 2, \dots, n$$

From now on, $\overline{\overline{\widehat{V}}_l^{(i)}}$ and $\overline{\overline{\widehat{I}}_l^{(i)}}$ will be used to represent voltage and current at the feeding plane of antenna l when antenna i is transmitting and

the rest are receiving. Substituting (8) into (18) yields

$$\sum_{l=1}^n \left[\overline{\widehat{a}_l^{(i)} \widehat{b}_l^{(j)}} - \overline{\widehat{a}_l^{(j)} \widehat{b}_l^{(i)}} \right] = 0$$

For a matched system, the above equation reduces to $\overline{\widehat{a}_i^{(i)} \widehat{b}_i^{(j)}} = \overline{\widehat{a}_j^{(j)} \widehat{b}_j^{(i)}}$, which gives the symmetric property of scattering matrix

$$S_{ij} = \overline{\widehat{b}_i^{(j)} / \widehat{a}_j^{(j)}} \Big|_{\overline{\widehat{a}_i^{(j)} = 0, i \neq j}} = \overline{\widehat{b}_j^{(i)} / \widehat{a}_i^{(i)}} \Big|_{\overline{\widehat{a}_j^{(i)} = 0, j \neq i}} = S_{ji} \quad (19)$$

Now choosing S as $S'_i + S_i$ in (17), where S'_i is a closed surface containing antenna i only, gives

$$\overline{\widehat{V}_i^{(i)} \widehat{I}_i^{(j)}} - \overline{\widehat{V}_i^{(j)} \widehat{I}_i^{(i)}} = \int_{S'_i} \left(\overline{\widehat{\mathbf{E}}_i \times \widehat{\mathbf{H}}_j} - \overline{\widehat{\mathbf{E}}_j \times \widehat{\mathbf{H}}_i} \right) \cdot \mathbf{u}_n ds \quad (20)$$

Similarly it may be found that

$$\overline{\widehat{V}_j^{(j)} \widehat{I}_j^{(i)}} - \overline{\widehat{V}_j^{(i)} \widehat{I}_j^{(j)}} = \int_{S'_j} \left(\overline{\widehat{\mathbf{E}}_j \times \widehat{\mathbf{H}}_i} - \overline{\widehat{\mathbf{E}}_i \times \widehat{\mathbf{H}}_j} \right) \cdot \mathbf{u}_n ds \quad (21)$$

where S'_j is a closed surface containing antenna j only. In terms of the normalized incident and reflected waves defined by (8), (20) and (21) can be written as

$$\overline{\widehat{b}_i^{(i)} \widehat{a}_i^{(j)}} - \overline{\widehat{b}_i^{(j)} \widehat{a}_i^{(i)}} = \frac{1}{2} \int_{S'_i} \left(\overline{\widehat{\mathbf{E}}_i \times \widehat{\mathbf{H}}_j} - \overline{\widehat{\mathbf{E}}_j \times \widehat{\mathbf{H}}_i} \right) \cdot \mathbf{u}_n ds \quad (22)$$

$$\overline{\widehat{b}_j^{(j)} \widehat{a}_j^{(i)}} - \overline{\widehat{b}_j^{(i)} \widehat{a}_j^{(j)}} = \frac{1}{2} \int_{S'_j} \left(\overline{\widehat{\mathbf{E}}_j \times \widehat{\mathbf{H}}_i} - \overline{\widehat{\mathbf{E}}_i \times \widehat{\mathbf{H}}_j} \right) \cdot \mathbf{u}_n ds \quad (23)$$

From (22) and (23), one may obtain

$$S_{ij} = \overline{\widehat{b}_i^{(j)} / \widehat{a}_j^{(j)}} \Big|_{\overline{\widehat{a}_i^{(j)} = 0, l \neq j}} = - \frac{1}{2 \overline{\widehat{a}_i^{(i)} \widehat{a}_j^{(j)}}} \int_{S'_i} \left(\overline{\widehat{\mathbf{E}}_i \times \widehat{\mathbf{H}}_j} - \overline{\widehat{\mathbf{E}}_j \times \widehat{\mathbf{H}}_i} \right) \cdot \mathbf{u}_n ds \quad (24)$$

$$S_{ji} = \overline{\widehat{b}_j^{(i)} / \widehat{a}_i^{(i)}} \Big|_{\overline{\widehat{a}_j^{(i)} = 0, l \neq i}} = - \frac{1}{2 \overline{\widehat{a}_i^{(i)} \widehat{a}_j^{(j)}}} \int_{S'_j} \left(\overline{\widehat{\mathbf{E}}_j \times \widehat{\mathbf{H}}_i} - \overline{\widehat{\mathbf{E}}_i \times \widehat{\mathbf{H}}_j} \right) \cdot \mathbf{u}_n ds \quad (25)$$

Note that (24) and (25) are exact and may be regarded as a different expression of Huygens' principle [33], which is applicable to an inhomogeneous medium. In fact, the effects of environments such as the scatters and the coupling between any two antenna elements have all been included in (24) and (25). The fields $\left\{ \overline{\overline{\mathbf{E}}}_i, \overline{\overline{\mathbf{H}}}_i \right\}$ should be determined with all antenna elements and scatters being in place.

4.1. Channel Matrix in Free Space

The computation of the fields $\left\{ \overline{\overline{\mathbf{E}}}_i, \overline{\overline{\mathbf{H}}}_i \right\}$ ($i = 1, 2, \dots, n$) in (24) with antenna j ($j \neq i$) and all scatters being in place is not an easy task, and one must resort to numerical methods in order to obtain the channel matrix elements S_{ij} . When the separations between antennas are large enough and all antennas are in free space (i.e., there are no scatters), the following simplification is usually made [30–32]: the calculation of $\left\{ \overline{\overline{\mathbf{E}}}_i, \overline{\overline{\mathbf{H}}}_i \right\}$ produced by antenna i is carried out with all other antennas removed. Physically this simplification is equivalent to neglecting the reflection between antennas. It will be assumed that the antennas are located in the far field region of each other. To derive the expressions of S_{ij} when the antenna i and antenna j are far apart, two different coordinate systems for antenna i and antenna j will be used. Let $2a_i$ be the maximum size of antenna i . The origins of the coordinate systems are chosen to be the geometrical center of the current distributions and the separation between antenna i and antenna j satisfies $kr_j \gg 1$, $r_j \gg 2a_j$, $r_j \gg 2a_i$ where $r_j = |\mathbf{r}_j|$ is the distance between antenna j and an arbitrary point of the circumscribing sphere (denoted by S'_i) of antenna i , as shown in Figure 4. Let \mathbf{r}'_i be a point on the circumscribing sphere of antenna i , and $\mathbf{r}_{i,j} = r_{i,j}\mathbf{u}_{r_{i,j}}$, where $r_{i,j}$ is the distance between the two origins and $\mathbf{u}_{r_{i,j}}$ is a unit vector directed from antenna i to antenna j . Thus the far field of antenna j at antenna i can be expressed as

$$\overline{\overline{\mathbf{E}}}_j(\mathbf{r}_j) \approx -\frac{jk\eta\widehat{\mathbf{I}}_j^{(j)}e^{-jkr_j}}{4\pi r_j}\mathbf{L}_j(\mathbf{u}_{r_j}), \quad \overline{\overline{\mathbf{H}}}_j(\mathbf{r}_j) \approx \frac{1}{\eta}\mathbf{u}_{r_j} \times \overline{\overline{\mathbf{E}}}_j(\mathbf{r}_j) \quad (26)$$

where $k = \omega_c\sqrt{\mu_0\varepsilon_0}$, $\eta = 120\pi$ is the wave impedance in free space, $\mathbf{r}_j = \mathbf{r}'_i - \mathbf{r}_{i,j}$ is assumed to be a point on the circumscribing sphere S'_i

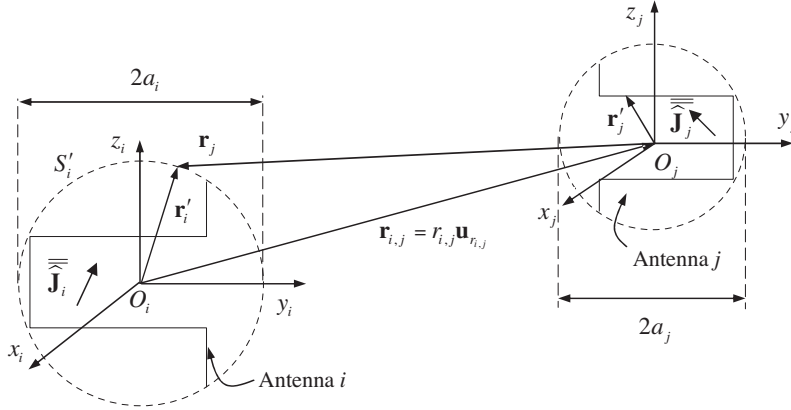


Figure 4. Coupling between two antenna elements in free space.

of antenna i , and

$$\mathbf{L}_j(\mathbf{u}_{r_j}) = \frac{1}{\widehat{I}_j^{(j)}} \int_{V_j} \left[\overline{\overline{\mathbf{J}}_j} - \left(\overline{\overline{\mathbf{J}}_j} \cdot \mathbf{u}_{r_j} \right) \mathbf{u}_{r_j} \right] e^{jk\mathbf{r}'_j \cdot \mathbf{u}_{r_j}} dv(\mathbf{r}'_j)$$

is the antenna effective vector length [30] with $\overline{\overline{\mathbf{J}}_j}$ being the current distribution and V_j being the source region of antenna j respectively. Since \mathbf{r}'_i is very small compared to $r_{i,j}$ in magnitude, one may make the approximation $r_j = |\mathbf{r}'_i - \mathbf{r}_{i,j}| \approx r_{i,j} - \mathbf{u}_{r_{i,j}} \cdot \mathbf{r}'_i$. The field $\overline{\overline{\mathbf{E}}_j}$ in the coordinate system O_i can then be written as

$$\begin{aligned} \overline{\overline{\mathbf{E}}_j}(\mathbf{r}_j) &\approx -\frac{jk\eta\widehat{I}_j^{(j)} e^{-jkr_{i,j}} e^{jk\mathbf{u}_{r_{i,j}} \cdot \mathbf{r}'_i}}{4\pi r_{i,j}} \mathbf{L}_j(-\mathbf{u}_{r_{i,j}}), \\ \overline{\overline{\mathbf{H}}_j}(\mathbf{r}_j) &\approx -\frac{1}{\eta} \mathbf{u}_{r_{i,j}} \times \overline{\overline{\mathbf{E}}_j}(\mathbf{r}_j) \end{aligned} \quad (27)$$

Then one may find that

$$\begin{aligned} &\int_{S'_i} \left(\overline{\overline{\mathbf{E}}_i} \times \overline{\overline{\mathbf{H}}_j} - \overline{\overline{\mathbf{E}}_j} \times \overline{\overline{\mathbf{H}}_i} \right) \cdot \mathbf{u}_n ds(\mathbf{r}'_i) \\ &= \int_{S'_i} \left[-\eta^{-1} \overline{\overline{\mathbf{E}}_i} \times \left(\mathbf{u}_{r_{i,j}} \times \overline{\overline{\mathbf{E}}_j} \right) - \overline{\overline{\mathbf{E}}_j} \times \overline{\overline{\mathbf{H}}_i} \right] \cdot \mathbf{u}_n ds(\mathbf{r}'_i) \end{aligned}$$

$$\begin{aligned}
&= \int_{S'_i} \overline{\overline{\mathbf{E}}_j} \cdot \left[-\eta^{-1} \mathbf{u}_{r_{i,j}} \times \left(\overline{\overline{\mathbf{E}}_i} \times \mathbf{u}_n \right) - \overline{\overline{\mathbf{H}}_i} \times \mathbf{u}_n \right] \cdot ds(\mathbf{r}'_i) \\
&= \int_{S'_i} \overline{\overline{\mathbf{E}}_j} \cdot \left(\overline{\overline{\mathbf{J}}_{is}} - \eta^{-1} \mathbf{u}_{r_{i,j}} \times \overline{\overline{\mathbf{J}}_{ims}} \right) ds(\mathbf{r}'_i) \quad (28)
\end{aligned}$$

where $\overline{\overline{\mathbf{J}}_{is}} = \mathbf{u}_n \times \overline{\overline{\mathbf{H}}_i}$, $\overline{\overline{\mathbf{J}}_{ims}} = -\mathbf{u}_n \times \overline{\overline{\mathbf{E}}_i}$. Substituting (27) into (28) gives

$$\int_{S'_i} \left(\overline{\overline{\mathbf{E}}_i} \times \overline{\overline{\mathbf{H}}_j} - \overline{\overline{\mathbf{E}}_j} \times \overline{\overline{\mathbf{H}}_i} \right) \cdot \mathbf{u}_n ds \approx \frac{-jk\eta \overline{\overline{\Gamma}}_i^{(i)} \overline{\overline{\Gamma}}_j^{(j)} e^{-jkr_{i,j}}}{4\pi r_{i,j}} \mathbf{L}_i(\mathbf{u}_{r_{i,j}}) \cdot \mathbf{L}_j(-\mathbf{u}_{r_{i,j}}) \quad (29)$$

where the far field expression of antenna i at antenna j

$$\begin{aligned}
\overline{\overline{\mathbf{E}}_i(\mathbf{r}_{i,j})} &= \frac{-jk\eta e^{-jkr_{i,j}}}{4\pi r_{i,j}} \int_{S'_i} e^{jk\mathbf{u}_{r_{i,j}} \cdot \mathbf{r}'_i} \left[\overline{\overline{\mathbf{J}}_{is}} - \mathbf{u}_{r_{i,j}} \times \frac{1}{\eta} \overline{\overline{\mathbf{J}}_{ims}} \right] ds(\mathbf{r}'_i) \\
&= \frac{-jk\eta \overline{\overline{\Gamma}}_i^{(i)} e^{-jkr_{i,j}}}{4\pi r_{i,j}} \mathbf{L}_i(\mathbf{u}_{r_{i,j}}) \quad (30)
\end{aligned}$$

has been used. From (8), (24) and (29) one may obtain (for a matched system)

$$\begin{aligned}
S_{ij} &\approx \frac{jk\eta \overline{\overline{\Gamma}}_i^{(i)} \overline{\overline{\Gamma}}_j^{(j)} e^{-jkr_{i,j}}}{8\pi r_{i,j} \overline{\overline{a}}_i^{(i)} \overline{\overline{a}}_j^{(j)}} \mathbf{L}_i(\mathbf{u}_{r_{i,j}}) \cdot \mathbf{L}_j(-\mathbf{u}_{r_{i,j}}) \\
&= \frac{jk\eta e^{-jkr_{i,j}}}{8\pi r_{i,j} \sqrt{\text{Re } Z_{si}} \sqrt{\text{Re } Z_{sj}}} \mathbf{L}_i(\mathbf{u}_{r_{i,j}}) \cdot \mathbf{L}_j(-\mathbf{u}_{r_{i,j}}) \quad (31)
\end{aligned}$$

(31) indicates that no coupling exists between two antenna elements if they are perpendicularly polarized.

4.2. Channel Matrix in a Scattering Environment

Unless the separations between the antenna elements are large enough, a MIMO system fails in free space. In fact the multi-path fading due to the scatters plays an important role in a MIMO system [20]. The

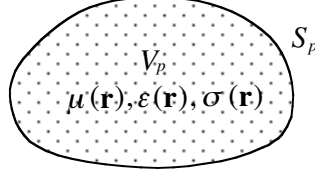


Figure 5. An arbitrary region where medium property changes.

presence of significant scatters in the propagation medium guarantees that the waves from different paths will add differently at each receiving antenna element so that the n_r receiving signals are independent, and can be used to unscramble the n_t transmitted signals. To predict how the MIMO channel matrix changes with environments, the general expression (24) or (25) can be used via numerical simulations with all scatters being in place. If the presence of the scatters does not change the field distributions significantly, a perturbation procedure may be adopted [33]. To this purpose a compensation theorem for electromagnetic fields will be introduced first, which claims that the influence of the medium on the fields can partly or completely be compensated by appropriate distribution of impressed currents [34]. Consider an arbitrary region V_p enclosed by a surface S_p in which the medium is assumed to be linear, isotropic and free of impressed source (Figure 5). The medium in V_p may be inhomogeneous with a permeability $\mu(\mathbf{r})$, permittivity $\varepsilon(\mathbf{r})$, and conductivity $\sigma(\mathbf{r})$. Thus one may write

$$\begin{cases} \nabla \times \overline{\overline{\mathbf{H}}}(\mathbf{r}) = [\sigma(\mathbf{r}) + j\omega_c\varepsilon(\mathbf{r})]\overline{\overline{\mathbf{E}}}(\mathbf{r}) + \overline{\overline{\mathbf{J}}}(\mathbf{r}) \\ \nabla \times \overline{\overline{\mathbf{E}}}(\mathbf{r}) = -j\omega_c\mu(\mathbf{r})\overline{\overline{\mathbf{H}}}(\mathbf{r}) \end{cases} \quad (32)$$

If the medium parameters $\mu(\mathbf{r}), \varepsilon(\mathbf{r}), \sigma(\mathbf{r})$ are changed to $\mu'(\mathbf{r}), \varepsilon'(\mathbf{r}), \sigma'(\mathbf{r})$ in V_p , the perturbed fields will be governed by

$$\begin{cases} \nabla \times \overline{\overline{\mathbf{H}'}}(\mathbf{r}) = [\sigma'(\mathbf{r}) + j\omega_c\varepsilon'(\mathbf{r})]\overline{\overline{\mathbf{E}'}}(\mathbf{r}) + \overline{\overline{\mathbf{J}'}}(\mathbf{r}) \\ \nabla \times \overline{\overline{\mathbf{E}'}}(\mathbf{r}) = -j\omega_c\mu'(\mathbf{r})\overline{\overline{\mathbf{H}'}}(\mathbf{r}) \end{cases} \quad \mathbf{r} \in V_p \quad (33)$$

which may be rewritten as

$$\begin{cases} \nabla \times \overline{\overline{\mathbf{H}'}}(\mathbf{r}) = [\sigma(\mathbf{r}) + j\omega_c\varepsilon(\mathbf{r})]\overline{\overline{\mathbf{E}'}}(\mathbf{r}) + \overline{\overline{\mathbf{J}'}}(\mathbf{r}) + \overline{\overline{\mathbf{J}}}(\mathbf{r}) \\ \nabla \times \overline{\overline{\mathbf{E}'}}(\mathbf{r}) = -j\omega_c\mu(\mathbf{r})\overline{\overline{\mathbf{H}'}}(\mathbf{r}) - \overline{\overline{\mathbf{J}_m}}(\mathbf{r}) \end{cases}, \quad \mathbf{r} \in V_p \quad (34)$$

where

$$\begin{cases} \overline{\overline{\widehat{\mathbf{J}}'}}(\mathbf{r}) = \{\sigma'(\mathbf{r}) - \sigma(\mathbf{r}) + j\omega_c[\varepsilon'(\mathbf{r}) - \varepsilon(\mathbf{r})]\}\overline{\overline{\widehat{\mathbf{E}}'}}(\mathbf{r}) \\ \overline{\overline{\widehat{\mathbf{J}}'_m}}(\mathbf{r}) = j\omega_c\overline{\overline{\widehat{\mathbf{H}}'}}(\mathbf{r})[\mu'(\mathbf{r}) - \mu(\mathbf{r})] \end{cases}, \quad \mathbf{r} \in V_p \quad (35)$$

Comparing (32) and (34), it may be found that the perturbed fields can be determined by introducing an equivalent electric current source $\overline{\overline{\widehat{\mathbf{J}}'}}(\mathbf{r})$ and an equivalent magnetic current source $\overline{\overline{\widehat{\mathbf{J}}'_m}}(\mathbf{r})$ in the region V_p , as if the medium parameters had not changed in V_p . This is what the compensation theorem implies. The differences of the fields $\Delta\overline{\overline{\widehat{\mathbf{E}}}}(\mathbf{r}) = \overline{\overline{\widehat{\mathbf{E}}'}}(\mathbf{r}) - \overline{\overline{\widehat{\mathbf{E}}}}(\mathbf{r})$, $\Delta\overline{\overline{\widehat{\mathbf{H}}}}(\mathbf{r}) = \overline{\overline{\widehat{\mathbf{H}}'}}(\mathbf{r}) - \overline{\overline{\widehat{\mathbf{H}}}}(\mathbf{r})$ satisfy the following equations

$$\begin{cases} \nabla \times \Delta\overline{\overline{\widehat{\mathbf{H}}}}(\mathbf{r}) = [\sigma(\mathbf{r}) + j\omega_c\varepsilon(\mathbf{r})]\Delta\overline{\overline{\widehat{\mathbf{E}}}}(\mathbf{r}) + \overline{\overline{\widehat{\mathbf{J}}'}}(\mathbf{r}) \\ \nabla \times \Delta\overline{\overline{\widehat{\mathbf{E}}}}(\mathbf{r}) = -j\omega_c\mu(\mathbf{r})\Delta\overline{\overline{\widehat{\mathbf{H}}}}(\mathbf{r}) - \overline{\overline{\widehat{\mathbf{J}}'_m}}(\mathbf{r}) \end{cases}, \quad (36)$$

Therefore the equivalent sources (35) generate the differential fields.

The influences of the change of the medium parameters on the scattering parameters can be studied by means of compensation theorem. Figure 6 shows any two antenna element i and j and a region V_p enclosed by S_p , where the changes of medium parameters take place. Two scenarios will be considered:

Scenario 1: The medium parameters are assumed to be μ, ε and σ .

The antenna i produces the fields $\overline{\overline{\widehat{\mathbf{E}}_i}}, \overline{\overline{\widehat{\mathbf{H}}_i}}$ when all other antennas are receiving. The transmission coefficient between antenna i and antenna j ($j \neq i$) is denoted by S_{ij} .

Scenario 2: The medium parameters μ, ε and σ in V_p are changed to μ', ε' and σ' respectively. The antenna i produces the field $\overline{\overline{\widehat{\mathbf{E}}'_i}}, \overline{\overline{\widehat{\mathbf{H}}'_i}}$ when all other antennas are receiving. The transmission coefficient between antenna i and antenna j ($j \neq i$) is denoted by S'_{ij} .

From (19), (24), (25) and the reciprocity theorem in a region with impressed sources [e.g., 29], the transmission coefficient for scenario 1 may be expressed as

$$\begin{aligned} S_{ij} &= -\frac{1}{2\widehat{a}_i^{(i)}\widehat{a}_j^{(j)}} \int_{S'_i} \left(\overline{\overline{\widehat{\mathbf{E}}_i}} \times \overline{\overline{\widehat{\mathbf{H}}_j}} - \overline{\overline{\widehat{\mathbf{E}}_j}} \times \overline{\overline{\widehat{\mathbf{H}}_i}} \right) \cdot \mathbf{u}_n ds \\ &= -\frac{1}{2\widehat{a}_i^{(i)}\widehat{a}_j^{(j)}} \int_{V'_j} \overline{\overline{\widehat{\mathbf{J}}_j}} \cdot \overline{\overline{\widehat{\mathbf{E}}_i}} dv \end{aligned} \quad (37)$$

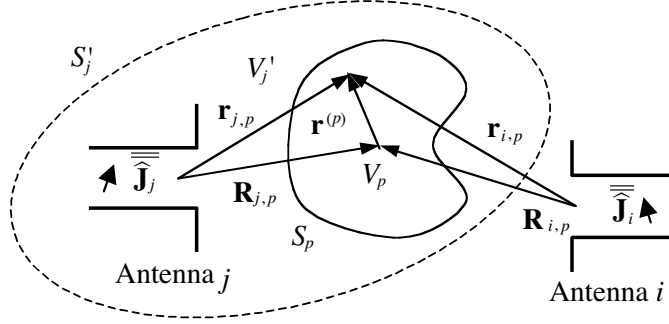


Figure 6. Coupling between two antenna elements in a scattering environment.

where S'_i is the surface enclosing antenna i only (V_p is not contained in S'_i) and V'_j is the region enclosed by S'_j , which contains both antenna j and V_p (Figure 6) and $\overline{\overline{\mathbf{J}}}_j$ is the current distribution of antenna j . Similarly the perturbed transmission coefficient for scenario 2 can be expressed as (assuming that the impressed $\overline{\overline{\mathbf{J}}}_j$ remains unchanged)

$$\begin{aligned} S'_{ij} &= -\frac{1}{2\hat{a}_i^{(i)}\hat{a}_j^{(j)}} \int_{S'_i} \left(\overline{\overline{\mathbf{E}}}_i \times \overline{\overline{\mathbf{H}}}_j - \overline{\overline{\mathbf{E}}}_j \times \overline{\overline{\mathbf{H}}}_i \right) \cdot \mathbf{u}_n ds \\ &= -\frac{1}{2\hat{a}_i^{(i)}\hat{a}_j^{(j)}} \int_{V'_j} \overline{\overline{\mathbf{J}}}_j \cdot \overline{\overline{\mathbf{E}}}_i dv \end{aligned} \quad (38)$$

Subtracting (37) from (38) gives

$$S'_{ij} - S_{ij} = -\frac{1}{2\hat{a}_i^{(i)}\hat{a}_j^{(j)}} \int_{V'_j} \overline{\overline{\mathbf{J}}}_j \cdot \left(\overline{\overline{\mathbf{E}}}_i' - \overline{\overline{\mathbf{E}}}_i \right) dv \quad (39)$$

Considering that V'_j contains the region V_p and the sources producing the differential fields $\Delta\overline{\overline{\mathbf{E}}} = \overline{\overline{\mathbf{E}}}' - \overline{\overline{\mathbf{E}}}$ and $\Delta\overline{\overline{\mathbf{H}}} = \overline{\overline{\mathbf{H}}}' - \overline{\overline{\mathbf{H}}}$ are given by (35), (39) may be written as

$$S'_{ij} - S_{ij} = -\frac{1}{2\hat{a}_i^{(i)}\hat{a}_j^{(j)}} \int_{V_p} \overline{\overline{\mathbf{J}}}' \cdot \overline{\overline{\mathbf{E}}}'_j - \overline{\overline{\mathbf{J}}}'_m \cdot \overline{\overline{\mathbf{H}}}'_j dv$$

$$\begin{aligned}
&= \frac{1}{2\widehat{a}_i^{(i)}\widehat{a}_j^{(j)}} \int_{V_p} \left\{ j\omega_c(\mu' - \mu) \overline{\overline{\mathbf{H}}}_i \cdot \overline{\overline{\mathbf{H}}}_j \right. \\
&\quad \left. - [\sigma' - \sigma + j\omega_c(\varepsilon' - \varepsilon)] \overline{\overline{\mathbf{E}}}_i \cdot \overline{\overline{\mathbf{E}}}_j \right\} dv \quad (40)
\end{aligned}$$

from the reciprocity theorem. This formula is useful to study the effect of changes in permittivity and permeability of the medium in a finite three dimensional region. But it is not convenient to study the changes in highly conducting bodies where the fields are confined to a shallow surface layer. In this case a surface integral will be more suitable. Making use of reciprocity theorem again, (40) may be expressed as

$$\begin{aligned}
S'_{ij} - S_{ij} &= -\frac{1}{2\widehat{a}_i^{(i)}\widehat{a}_j^{(j)}} \int_{V_p} \overline{\overline{\mathbf{J}}}' \cdot \overline{\overline{\mathbf{E}}}_j - \overline{\overline{\mathbf{J}}}'_m \cdot \overline{\overline{\mathbf{H}}}_j dv \\
&= -\frac{1}{2\widehat{a}_i^{(i)}\widehat{a}_j^{(j)}} \int_{S_p} \left[\left(\overline{\overline{\mathbf{E}}}'_i - \overline{\overline{\mathbf{E}}}_i \right) \times \overline{\overline{\mathbf{H}}}_j - \overline{\overline{\mathbf{E}}}_j \times \left(\overline{\overline{\mathbf{H}}}'_i - \overline{\overline{\mathbf{H}}}_i \right) \right] \cdot \mathbf{u}_n ds \\
&= \frac{1}{2\widehat{a}_i^{(i)}\widehat{a}_j^{(j)}} \int_{S_p} \left(\overline{\overline{\mathbf{E}}}_j \times \overline{\overline{\mathbf{H}}}'_i - \overline{\overline{\mathbf{E}}}'_j \times \overline{\overline{\mathbf{H}}}_i \right) \cdot \mathbf{u}_n ds \quad (41)
\end{aligned}$$

Note that only the field components tangential to S_p contributes to (41). Let Z_s and Z'_s be the surface impedances before and after the change of the medium parameters respectively. Considering the relations $\overline{\overline{\mathbf{E}}}'_{jt} = Z_s \mathbf{u}_n \times \overline{\overline{\mathbf{H}}}_{it}$, $\overline{\overline{\mathbf{E}}}'_{jt} = Z'_s \mathbf{u}_n \times \overline{\overline{\mathbf{H}}}'_{it}$, (41) may be rewritten as

$$S'_{ij} - S_{ij} = \frac{1}{2\widehat{a}_i^{(i)}\widehat{a}_j^{(j)}} \int_{S_p} (Z'_s - Z_s) \overline{\overline{\mathbf{H}}}'_{jt} \cdot \overline{\overline{\mathbf{H}}}_{it} ds \quad (42)$$

where the subscript t is used to represent the tangential component.

If there exist m scatters and each scatter occupies a region V_p ($p = 1, 2, \dots, m$), then the integrations in (40)–(42) become a summation of integrations over each scatter. For instance, (40) may be written as

$$\begin{aligned}
S'_{ij} &= S_{ij} + \frac{1}{2\widehat{a}_i^{(i)}\widehat{a}_j^{(j)}} \sum_{p=1}^m \int_{V_p} \left\{ j\omega_c(\mu' - \mu) \overline{\overline{\mathbf{H}}}_i \cdot \overline{\overline{\mathbf{H}}}_j \right. \\
&\quad \left. - [\sigma' - \sigma + j\omega_c(\varepsilon' - \varepsilon)] \overline{\overline{\mathbf{E}}}_i \cdot \overline{\overline{\mathbf{E}}}_j \right\} dv \quad (43)
\end{aligned}$$

The first term of (43) corresponds to the contribution due to the direct path from antenna i to antenna j . The second term represents the m multipath components introduced by the m scatters and usually improve the condition number of the channel matrix $\underline{\mathbf{H}}$, which is important for a wireless MIMO system to be effective.

So far our discussion is exact. If the parameters ξ_1 and ξ_2 defined by

$$\begin{cases} \xi_1 = \sigma'(\mathbf{r}) - \sigma(\mathbf{r}) + j\omega_c[\varepsilon'(\mathbf{r}) - \varepsilon(\mathbf{r})] \\ \xi_2 = j\omega_c[\mu'(\mathbf{r}) - \mu(\mathbf{r})] \end{cases}$$

are small numbers, a perturbation method may be introduced to predict S'_{ij} [33]. In this case, the fields $\overline{\overline{\mathbf{E}}}_i$ and $\overline{\overline{\mathbf{H}}}_i$ may be expanded in terms of ξ_1 and ξ_2 as follows

$$\begin{cases} \overline{\overline{\mathbf{E}}}_i = \overline{\overline{\mathbf{E}}}_i + \xi_1 \overline{\overline{\mathbf{E}}}_{i1} + \xi_2 \overline{\overline{\mathbf{E}}}_{i2} + \dots \\ \overline{\overline{\mathbf{H}}}_i = \overline{\overline{\mathbf{H}}}_i + \xi_1 \overline{\overline{\mathbf{H}}}_{i1} + \xi_2 \overline{\overline{\mathbf{H}}}_{i2} + \dots \end{cases}$$

As a first order approximation, (40), (41) and (42) can then be approximated by

$$\begin{aligned} S'_{ij} - S_{ij} \approx & \frac{1}{2\widehat{a}_i^{(i)}\widehat{a}_j^{(j)}V_p} \int \left\{ j\omega_c(\mu' - \mu) \overline{\overline{\mathbf{H}}}_i \cdot \overline{\overline{\mathbf{H}}}_j \right. \\ & \left. - [\sigma' - \sigma + j\omega_c(\varepsilon' - \varepsilon)] \overline{\overline{\mathbf{E}}}_i \cdot \overline{\overline{\mathbf{E}}}_j \right\} dv \end{aligned} \quad (44)$$

$$S'_{ij} - S_{ij} \approx \frac{1}{2\widehat{a}_i^{(i)}\widehat{a}_j^{(j)}S_p} \int \left(\overline{\overline{\mathbf{E}}}_j \times \overline{\overline{\mathbf{H}}}_i - \overline{\overline{\mathbf{E}}}_i \times \overline{\overline{\mathbf{H}}}_j \right) \cdot \mathbf{u}_n ds \quad (45)$$

$$S'_{ij} - S_{ij} \approx \frac{1}{2\widehat{a}_i^{(i)}\widehat{a}_j^{(j)}S_p} \int (Z'_s - Z_s) \overline{\overline{\mathbf{H}}}_{jt} \cdot \overline{\overline{\mathbf{H}}}_{it} ds \quad (46)$$

4.3. Numerical and Experimental Results

Let us consider a situation where the scenario 1 corresponds to the free space. Neglecting the reflections between antennas, the fields in the region V_p produced by antenna i and antenna j in free space may then

be approximated by

$$\begin{aligned}\overline{\overline{\widehat{\mathbf{E}}_i(\mathbf{r}_{i,p})}} &\approx -\frac{jk\eta\widehat{I}_i^{(i)}e^{-jkr_{i,p}}}{4\pi r_{i,p}}\mathbf{L}_i(\mathbf{u}_{r_{i,p}}), \\ \overline{\overline{\widehat{\mathbf{E}}_j(\mathbf{r}_{j,p})}} &\approx -\frac{jk\eta\widehat{I}_j^{(j)}e^{-jkr_{j,p}}}{4\pi r_{j,p}}\mathbf{L}_j(\mathbf{u}_{r_{j,p}})\end{aligned}\quad (47)$$

where $\mathbf{r}_{i,p} = r_{i,p}\mathbf{u}_{r_{i,p}}$ and $\mathbf{r}_{j,p} = r_{j,p}\mathbf{u}_{r_{j,p}}$ are observation points in V_p from antenna i and antenna j respectively (Figure 6). The transmission coefficient S_{ij} in scenario 1 is given by (31). In scenario 2, a dielectric scatter with dielectric constant $\varepsilon_p = \varepsilon_{rp}\varepsilon_0$ is introduced in region V_p . Substituting (47) into (44) and assuming the region V_p is in the far field region of both antenna i and antenna j one obtains

$$S'_{ij} - S_{ij} \approx \frac{jk^3\eta}{32\pi^2} \frac{\varepsilon_{rp} - 1}{\sqrt{\text{Re } Z_{si}}\sqrt{\text{Re } Z_{sj}}} \int_{V_p} \mathbf{L}_i(\mathbf{u}_{r_{i,p}}) \cdot \mathbf{L}_j(\mathbf{u}_{r_{j,p}}) \frac{e^{-jk(r_{i,p}+r_{j,p})}}{r_{i,p}r_{j,p}} dv(\mathbf{r}^{(p)}) \quad (48)$$

where the local coordinate system $\mathbf{r}^{(p)} = (x^{(p)}, y^{(p)}, z^{(p)})$ has been introduced and the transmission coefficient S_{ij} is approximated by (31). If there exist m dielectric scatters and each scatter occupies a region V_p ($p = 1, 2, \dots, m$), the above equation should change to

$$\begin{aligned}S'_{ij} &\approx \frac{jk\eta e^{-jkr_{i,j}}}{8\pi r_{i,j}} \frac{\mathbf{L}_i(\mathbf{u}_{r_{i,j}}) \cdot \mathbf{L}_j(-\mathbf{u}_{r_{i,j}})}{\sqrt{\text{Re } Z_{si}}\sqrt{\text{Re } Z_{sj}}} \\ &+ \frac{jk^3\eta}{32\pi^2} \frac{\varepsilon_{rp} - 1}{\sqrt{\text{Re } Z_{si}}\sqrt{\text{Re } Z_{sj}}} \sum_{p=1}^m (\varepsilon_{rp} - 1) \\ &\times \int_{V_p} \mathbf{L}_i(\mathbf{u}_{r_{i,p}}) \cdot \mathbf{L}_j(\mathbf{u}_{r_{j,p}}) \frac{e^{-jk(r_{i,p}+r_{j,p})}}{r_{i,p}r_{j,p}} dv(\mathbf{r}^{(p)})\end{aligned}\quad (49)$$

4.3.1. A Two-dipole System

To demonstrate (49), let us consider a two-dipole antenna system shown in Figure 7. The two dipoles will be assumed to be identical and are located in the far field region of each other. The length of the dipoles is $2a$ and the dipole current distribution is assumed to be $\widehat{I}(z_l) = \widehat{I}_0 \sin k(a - |z_l|)$, $|z_l| \leq a$ ($l = 1, 2$) [30]. The radiation

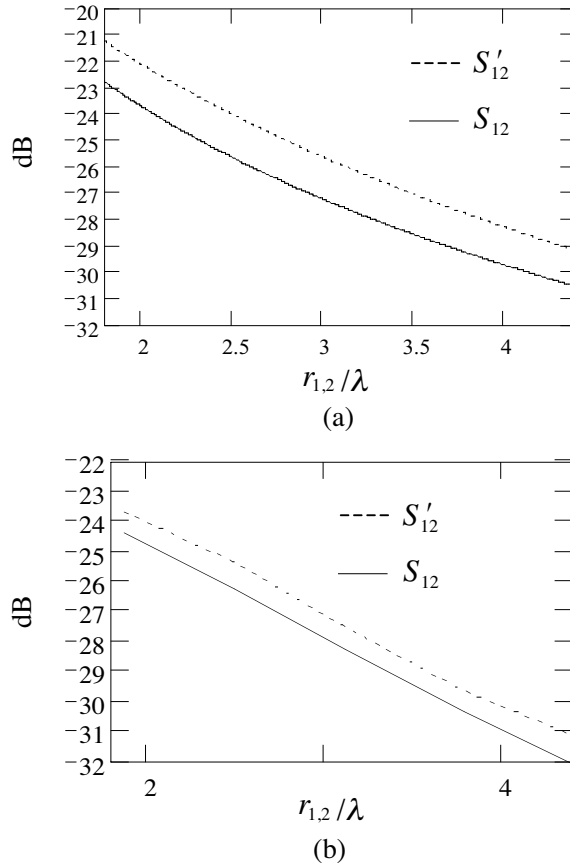


Figure 8. Transmission coefficient S_{12} (a) Theoretical predictions; (b) Experimental results ($\varepsilon_r = 4.4$, $a = 0.25\lambda$, $b_{xp} = 0.011\lambda$, $b_{yp} = b_{zp} = 0.5\lambda$).

In scenario 2, a dielectric slab with dielectric constant $\varepsilon = \varepsilon_r \varepsilon_0$ are introduced into the two-dipole system, as shown in Figure 7. The side lengths the dielectric slab are denoted by $2b_{xp}$, $2b_{yp}$ and $2b_{zp}$ respectively. The center of the dielectric slab is located at the middle of the two-dipole system. From the perturbation theory, the transmission coefficient between dipole 1 and dipole 2 can be obtained from (49) by letting $m = 1$.

The theoretical predictions in terms of (31) and (49) have been depicted as a function of separation between the two half-wavelength dipoles in Figure 8(a). Note that both (50) and (51) are based on

a delta gap approximation and the feeding line has been ignored. In this case the reference impedance are chosen as the conjugate of the input impedance of the dipole, i.e., $\text{Re } Z_{s1} = \text{Re } Z_{s2} = 73\Omega$ to comply with the general definition of the scattering parameters. To verify the theoretical predictions, two calibrated half-wavelength dipoles (ETS 3126-1880) matched to 50Ω (In this case the reference impedance is the characteristic impedance of the feeding coaxial cable) have been used to replace the two ideal dipoles and the measurement results are shown in Figure 8(b). Both theoretical predictions and experiments indicate that the introduction of the dielectric slab will enhance the coupling between the two-dipole system. Physically this can be explained as the focusing effect of the dielectric slab.

4.3.2. A 2×2 Dipole System

Next let us consider a 2×2 half-wavelength dipole system shown in Figure 9, where dipole 1 and dipole 2 form a transmitting array while dipole 3 and dipole 4 form a receiving array. The four dipoles are identical to the ones used in the previous two-dipole system. The separation between the two dipoles in the transmitting array is equal to the separation between the two dipoles in the receiving array, which is assumed to be half wavelength. The receiving array will be assumed in the far field region of transmitting array.

Let scenario 1 correspond to the 2×2 dipole system in free space

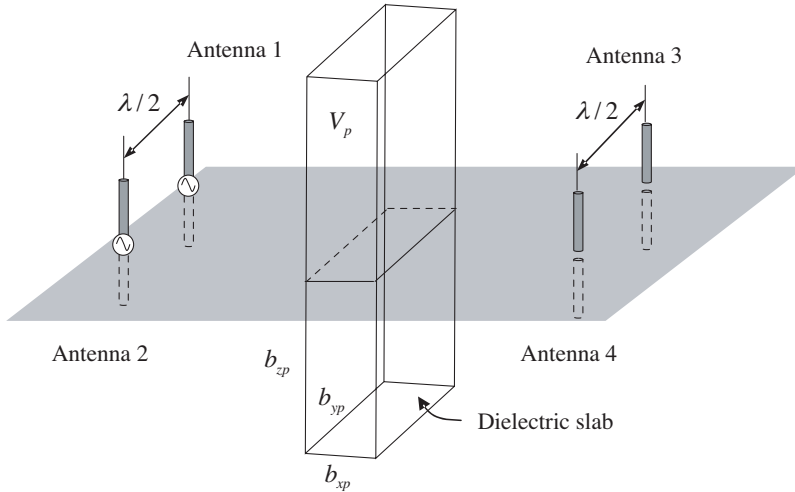


Figure 9. Influence of dielectric slab — A 2×2 system.

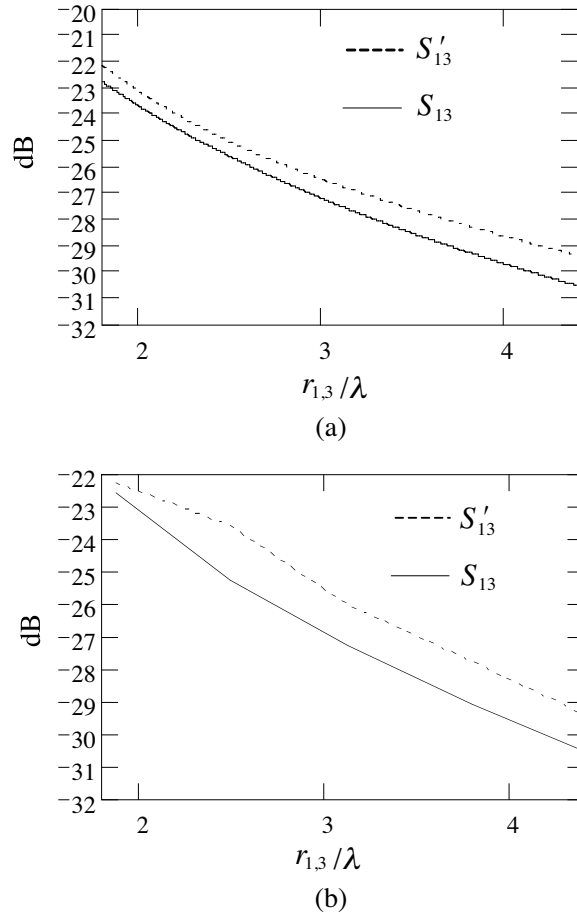


Figure 10. Transmission coefficient S_{13} (a) Theoretical predictions; (b) Experimental results ($\varepsilon_r = 4.4$, $a = 0.25\lambda$, $b_{xp} = 0.02\lambda$, $b_{yp} = b_{zp} = 0.5\lambda$).

with $\mu = \mu_0$, $\varepsilon = \varepsilon_0$ and $\sigma = 0$. In scenario 2, a dielectric slab of side lengths $(2b_{xp}, 2b_{yp}, 2b_{zp})$ with dielectric constant $\varepsilon = \varepsilon_r \varepsilon_0$ are introduced in the middle of the 2×2 system, as shown in Figure 9. The theoretical predictions of S_{13} and S_{14} based on (31) and (49) have been shown in Figure 10 (a) and Figure 11(a) and the measurement results are shown in Figure 10(b) and Figure 11(b). Note that the reference impedance has been chosen as the conjugate of the input impedance of the half-wavelength dipole in the theoretical calculation. In experiments, four calibrated half-wavelength dipoles (ETS 3126-

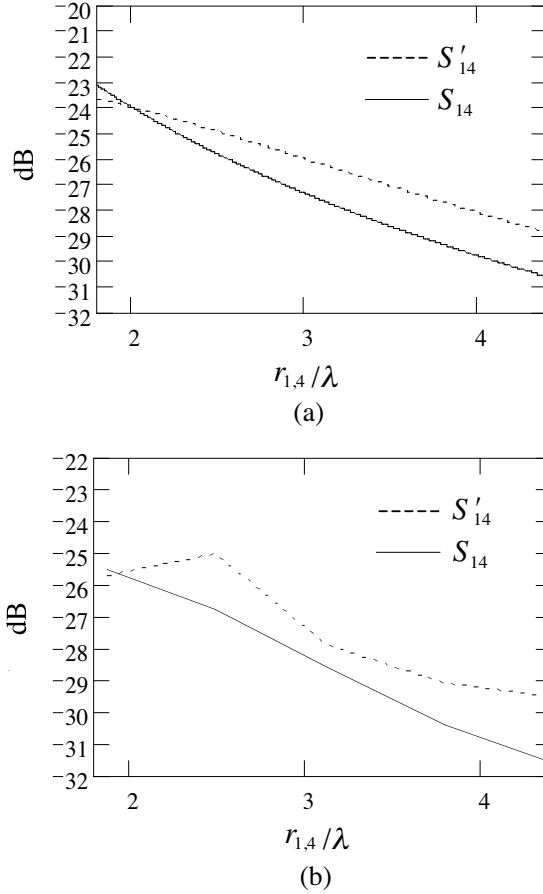


Figure 11. Transmission coefficient S_{14} (a) Theoretical predictions; (b) Experimental results ($\varepsilon_r = 4.4$, $a = 0.25\lambda$, $b_{xp} = 0.02\lambda$, $b_{yp} = b_{zp} = 0.5\lambda$).

1880) have been used and the reference impedance is 50Ω . Again one can see that the introduction of a dielectric slab will enhance the coupling between antennas.

5. UPPER BOUNDS OF INFORMATION CAPACITY

The most general upper bounds of capacity of a MIMO system have been given in (15) and (16). Now these general upper bounds will be applied to MIMO system in free space. In order to find the upper

bounds of the capacity of the MIMO system, one must know the upper limit of the antenna performances.

5.1. The Best Possible Antenna Performance

The antenna performance is usually characterized by gain G , fractional bandwidth B (the fractional bandwidth at the frequency ω_c is defined by $B = \Delta\omega/\omega_c$, where $\Delta\omega$ is the frequency increment between 0.707 points of the normalized input impedance) or quality factor Q_{real} . The latter is defined by [35, 36]

$$Q_{real} = \omega\tilde{W}/P \quad (52)$$

where \tilde{W} is the time average energy stored in the system and P is the average radiated power. Here a subscript ‘real’ is used to indicate that all stored energy around antenna has been included in the calculation of antenna quality factor, to distinguish it from another antenna quality factor, denoted by Q , to be introduced later, in which only the stored energy outside the circumscribing sphere of the antenna is used. Chu and Harrington have derived that the gain for an omni-directional antenna and directional antenna are bounded respectively by [17, 18]

$$G|_{omn} \leq \sum_{n=1,3,5\dots}^N \frac{(2n+1)|P_n^1(0)|^2}{n(n+1)}, \quad G|_{dir} \leq N(N+2) \quad (53)$$

Here N is the number of terms in the spherical wave function expansions, and the subscripts “*omn*” and “*dir*” refer to omni-directional antenna and directional antenna respectively. Therefore the upper bounds of the gain increase as N increases. Since the upper bounds on the gain given by (53) are independent of antenna size, one can, theoretically, achieve an arbitrarily large gain with an arbitrarily small antenna. However an antenna with extremely high gain is impractical as it would have high quality factor, leading to high conduction loss. To get a finite upper bound on the antenna gain, the concept of normal gain has been introduced [17, 18].

A more useful performance index for characterizing antenna is the product of antenna gain and bandwidth as they must be maximized simultaneously in most applications. It is known that the antenna fractional bandwidth is reciprocal to antenna Q_{real} if Q_{real} is not very small [36]. Therefore the product of antenna gain and bandwidth can be expressed as

$$GB \approx G/Q_{real} \quad (54)$$

Since any practical antenna can be classified into omni-directional and directional antenna in terms of their radiation patterns, it will be sufficient to consider the best possible antenna performances for these two general situations. To this purpose, another antenna quality factor, denoted by Q , is often introduced. This antenna Q is still defined by (52), but with \tilde{W} being replaced by the stored energy outside the circumscribing sphere of the antenna [17–19, 35]. It can be shown that the ratios of gain G to Q for an arbitrary omni-directional antenna and an arbitrary directional antenna whose maximum size is $2a$ are bounded respectively by [19]

$$G/Q \Big|_{omn} \leq \rho(ka) \Big|_{omn}, \quad G/Q \Big|_{dir} \leq \rho(ka) \Big|_{dir} \quad (55)$$

where

$$\begin{aligned} \rho(ka) \Big|_{omn} &= \sum_{n=1}^{\infty} \frac{2(2n+1) |P_n^1(0)|^2}{n(n+1)[Q_n(ka) + Q'_n(ka)]} \\ \rho(ka) \Big|_{dir} &= \sum_{n=1}^{\infty} \frac{2(2n+1)}{[Q_n(ka) + Q'_n(ka)]} \end{aligned} \quad (56)$$

with

$$\begin{aligned} Q_n(ka) &= ka - \left| h_n^{(2)}(ka) \right|^2 [(ka)^3/2 + ka(n+1)] - (ka)^3 \left| h_{n+1}^{(2)}(ka) \right|^2 / 2 \\ &\quad + (ka)^2 (2n+3) [j_n(ka)j_{n+1}(ka) + n_n(ka)n_{n+1}(ka)] / 2 \\ Q'_n(ka) &= ka - (ka)^3 \left[\left| h_n^{(2)}(ka) \right|^2 - j_{n-1}(ka)j_{n+1}(ka) \right. \\ &\quad \left. - n_{n-1}(ka)n_{n+1}(ka) \right] / 2 \end{aligned}$$

In the above, P_n^1 is the first associated Legendre polynomial; k is the wavenumber; $h_n^{(2)}$ and j_n are the spherical Hankel function of the second kind and the spherical Bessel function of the first kind respectively. Since the antenna Q in (55) does not include the stored energy inside the circumscribing sphere, it is smaller than the real antenna Q_{real} as the latter contains all the stored energy. Thus from (54) and (55), the products of antenna gain and bandwidth for an arbitrary omni-directional antenna and an arbitrary directional antenna are bounded respectively by

$$GB \Big|_{omn} \leq \rho(ka) \Big|_{omn}, \quad GB \Big|_{dir} \leq \rho(ka) \Big|_{dir} \quad (57)$$

Physically (57) implies that the product of antenna gain and bandwidth that can be achieved by an arbitrary antenna of maximum dimension $2a$ will never exceed the number given by the right-hand sides of the two inequalities in (57), and they also indicate that there is a tradeoff between antenna gain and bandwidth once the maximum antenna size is fixed. It should be notified that the right-hand sides of the two inequalities in (57) are finite numbers. Hence the maximum possible antenna gain is a finite number once the antenna bandwidth is specified, instead of an infinite number given by (53). Similarly the maximum possible antenna bandwidth is also finite once the antenna gain is specified. For small antennas with $ka < 1$, only the first term in (56) is significant. Thus (57) reduces to [19]

$$GB\Big|_{omn} \leq \frac{3}{Q_1 + Q'_1} = \frac{3(ka)^3}{2(ka)^2 + 1}, \quad GB\Big|_{dir} \leq \frac{6}{Q_1 + Q'_1} = \frac{6(ka)^3}{2(ka)^2 + 1} \quad (58)$$

The right-hand sides of the two inequalities in (58) are the best possible antenna performances that a small antenna of maximum dimension $2a$ can achieve. They can serve as a target that may be approached by various methods and have been proven to be very useful for small antenna design for which try and error method is often used. Once the antenna performance (product of the gain and bandwidth) is specified, (57)–(58) can be used to determine the antenna size required to achieve the performance specified. For example, one may obtain

$$GB\Big|_{omn} \leq \frac{3(ka)^3}{2(ka)^2 + 1} \approx 3(ka)^3 \quad (59)$$

from the first expression of (58) for $ka \ll 1$. If the product $GB\Big|_{omn}$ is given, the antenna size must be greater than $k^{-1} \sqrt[3]{GB\Big|_{omn}/3}$. It can be shown that the fractional bandwidth of an arbitrary small antenna of dimension $2a$ has an upper bound [19]

$$B \leq 2(ka)^3/[2(ka)^2 + 1]$$

To approach the upper bound of the bandwidth, one should use the space as efficiently as possible. When the upper bound of the bandwidth has been reached, it can be seen from (58) that the maximum possible antenna gain is 3 (4.8 dBi) for a directional small antenna and 1.5 (1.8 dBi) for an omni-directional small antenna.

5.2. Upper Bounds of Information Capacity

For simplicity all antennas will be assumed to be conjugately matched with $\text{Re } Z_{si} = R_i^{\text{rad}}$. Inserting (31) into (15) and (16) produces

$$\begin{aligned}
C &\leq \sum_{j=1}^{n_t} \log_2 \left[1 + \frac{P}{\sigma^2 n_t} \frac{k^2 \eta^2}{64\pi^2} \sum_{i=1}^{n_r} \frac{|\mathbf{L}_{n_t+i}(\mathbf{u}_{r_{n_t+i,j}}) \cdot \mathbf{L}_j(-\mathbf{u}_{r_{n_t+i,j}})|^2}{R_{n_t+i}^{\text{rad}} R_j^{\text{rad}} r_{n_t+i,j}^2} \right] \\
&\leq \sum_{j=1}^{n_t} \log_2 \left[1 + \frac{P}{\sigma^2 n_t} \frac{k^2 \eta^2}{64\pi^2} \sum_{i=1}^{n_r} \frac{|\mathbf{L}_{n_t+i}(\mathbf{u}_{r_{n_t+i,j}})|^2 |\mathbf{L}_j(-\mathbf{u}_{r_{n_t+i,j}})|^2}{R_{n_t+i}^{\text{rad}} R_j^{\text{rad}} r_{n_t+i,j}^2} \right] \\
&= \sum_{j=1}^{n_t} \log_2 \left[1 + \frac{P}{4\sigma^2 k^2 n_t} \sum_{i=1}^{n_r} \frac{G_j(-\mathbf{u}_{r_{n_t+i,j}}) G_{n_t+i}(\mathbf{u}_{r_{n_t+i,j}})}{r_{n_t+i,j}^2} \right] \quad (60)
\end{aligned}$$

and

$$\begin{aligned}
C &\leq \sum_{j=1}^{n_r} \log_2 \left[1 + \frac{P}{\sigma^2 n_t} \frac{k^2 \eta^2}{64\pi^2} \sum_{i=1}^{n_t} \frac{|\mathbf{L}_{n_t+j}(\mathbf{u}_{r_{n_t+j,i}}) \cdot \mathbf{L}_j(-\mathbf{u}_{r_{n_t+j,i}})|^2}{R_{n_t+j}^{\text{rad}} R_i^{\text{rad}} r_{n_t+j,i}^2} \right] \\
&\leq \sum_{j=1}^{n_r} \log_2 \left[1 + \frac{P}{\sigma^2 n_t} \frac{k^2 \eta^2}{64\pi^2} \sum_{i=1}^{n_t} \frac{|\mathbf{L}_{n_t+j}(\mathbf{u}_{r_{n_t+j,i}})|^2 |\mathbf{L}_j(-\mathbf{u}_{r_{n_t+j,i}})|^2}{R_{n_t+j}^{\text{rad}} R_i^{\text{rad}} r_{n_t+j,i}^2} \right] \\
&= \sum_{j=1}^{n_r} \log_2 \left[1 + \frac{P}{4\sigma^2 k^2 n_t} \sum_{i=1}^{n_t} \frac{G_{n_t+j}(\mathbf{u}_{r_{n_t+j,i}}) G_i(-\mathbf{u}_{r_{n_t+j,i}})}{r_{n_t+j,i}^2} \right] \quad (61)
\end{aligned}$$

where G_i is the directivity of antenna i ($i = 1, 2, \dots, n_t + n_r$). In deriving (60) and (61), the relation $G_i = \eta |k \mathbf{L}_i|^2 / 4\pi R_i^{\text{rad}}$ has been used. The right-hand sides of (60) and (61) are the upper bounds of the capacity for the MIMO system in free space and will be denoted by

$$C_m = \sum_{j=1}^{n_t} \log_2 \left[1 + \frac{P}{4\sigma^2 k^2 n_t} \sum_{i=1}^{n_r} \frac{G_j(-\mathbf{u}_{r_{n_t+i,j}}) G_{n_t+i}(\mathbf{u}_{r_{n_t+i,j}})}{r_{n_t+i,j}^2} \right] \quad (62)$$

and

$$C'_m = \sum_{j=1}^{n_r} \log_2 \left[1 + \frac{P}{4\sigma^2 k^2 n_t} \sum_{i=1}^{n_t} \frac{G_{n_t+j}(\mathbf{u}_{r_{n_t+j,i}}) G_i(-\mathbf{u}_{r_{n_t+j,i}})}{r_{n_t+j,i}^2} \right] \quad (63)$$

respectively. Now C_m and C'_m can be further maximized by optimizing the geometry of antennas under the constraint that the maximum sizes

of all antennas are fixed. From (62) and (63), maximizing C_m and C'_m is equivalent to maximizing antenna gain. From (57) it can be seen that the antenna gain could be as large as one wishes if the antenna bandwidth is allowed to be infinitely small. Therefore the antenna gain should be maximized with a specified antenna bandwidth as an antenna with very small bandwidth is a useless property in practice. Let us consider the maximization of (62). Introducing (57) into the right-hand side of (62) yields the upper bounds of capacity, denoted by $\max C_m$, for four different arrangements:

- Both transmitting antennas and receiving antennas are directional

$$\max C_m|_{d-d} = \sum_{j=1}^{n_t} \log_2 \left[1 + \frac{P}{4\sigma^2 k^2 n_t} \sum_{i=1}^{n_r} \frac{\rho(ka_j)|_{dir} \rho(ka_{n_t+i})|_{dir}}{B_j B_{n_t+i} r_{n_t+i,j}^2} \right] \quad (64)$$

- Both transmitting antennas and receiving antennas are omni-directional

$$\max C_m|_{o-o} = \sum_{j=1}^{n_t} \log_2 \left[1 + \frac{P}{4\sigma^2 k^2 n_t} \sum_{i=1}^{n_r} \frac{\rho(ka_j)|_{omn} \rho(ka_{n_t+i})|_{omn}}{B_j B_{n_t+i} r_{n_t+i,j}^2} \right] \quad (65)$$

- Transmitting antennas are directional while receiving antennas are omni-directional

$$\max C_m|_{d-o} = \sum_{j=1}^{n_t} \log_2 \left[1 + \frac{P}{4\sigma^2 k^2 n_t} \sum_{i=1}^{n_r} \frac{\rho(ka_j)|_{dir} \rho(ka_{n_t+i})|_{omn}}{B_j B_{n_t+i} r_{n_t+i,j}^2} \right] \quad (66)$$

- Transmitting antennas are omni-directional while receiving antennas are directional

$$\max C_m|_{o-d} = \sum_{j=1}^{n_t} \log_2 \left[1 + \frac{P}{4\sigma^2 k^2 n_t} \sum_{i=1}^{n_r} \frac{\rho(ka_j)|_{omn} \rho(ka_{n_t+i})|_{dir}}{B_j B_{n_t+i} r_{n_t+i,j}^2} \right] \quad (67)$$

In (64)–(67), $2a_i$ and B_i represent the maximum dimension and the fractional bandwidth of antenna i ($i = 1, 2, \dots, n_t + n_r$) respectively. Similar upper bounds can be obtained for C'_m . Once the required capacity is specified, (64)–(67) can be used to determine the antenna sizes required to achieve the capacity. Now some special MIMO systems will be discussed.

5.2.1. SISO System

Consider a SISO system consisting of antenna 1 and antenna 2 shown in Figure 12, where antenna 1 is transmitting and antenna 2 is receiving. In this case (62) reduces to

$$C_m = \log_2 \left[1 + \frac{P}{4\sigma^2 k^2} \frac{G_1(\mathbf{u}_{r_{1,2}})G_2(-\mathbf{u}_{r_{1,2}})}{r_{1,2}^2} \right] \quad (68)$$

The upper bounds of information capacities as a function of maximum antenna size for the SISO systems have been depicted in Figures 13–15, where $p/\sigma^2 = 20$ dB, $k = 1$ and $a_1 = a_2 = a$. It can be seen that the upper bounds of information capacities

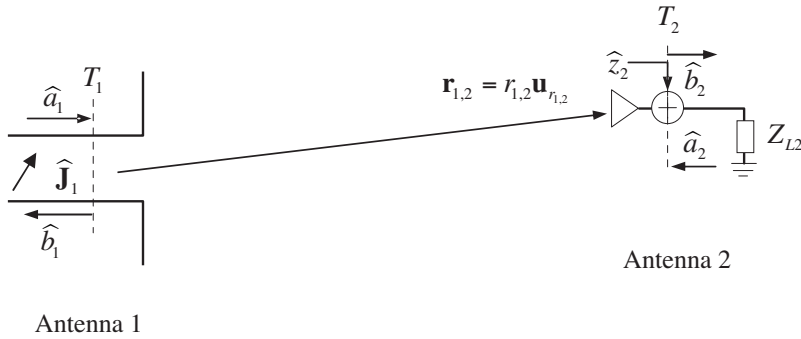


Figure 12. A SISO system.

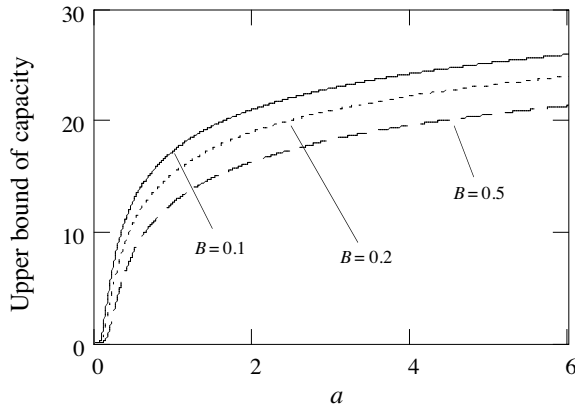


Figure 13. $\max C_m|_{d-d}$ ($k = 1$, $a_1 = a_2$, $B_1 = B_2$, $p/\sigma^2 = 20$ dB).

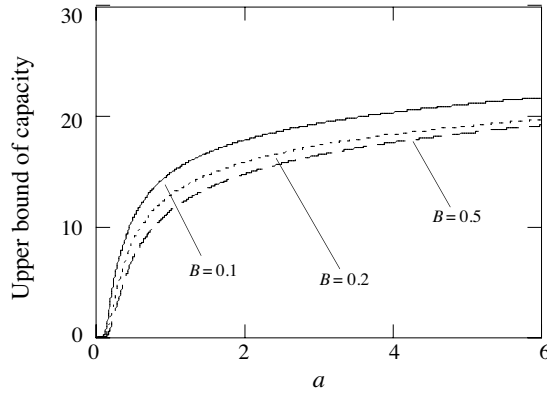


Figure 14. $\max C_m|_{o-o}$ ($k = 1, a_1 = a_2, B_1 = B_2, p/\sigma^2 = 20$ dB).

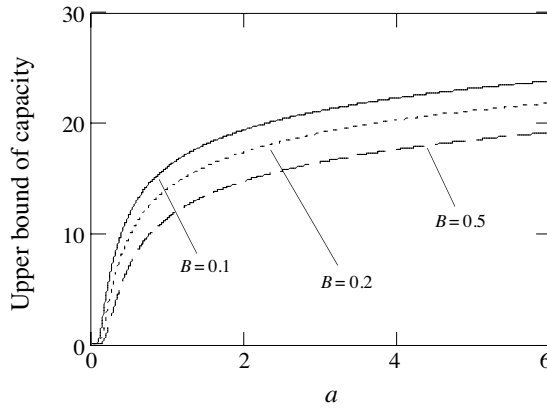


Figure 15. $\max C_m|_{d-o}$ ($k = 1, a_1 = a_2, B_1 = B_2, p/\sigma^2 = 20$ dB).

are a monotonically increasing function of the maximum antenna size a but a monotonically decreasing function of fractional antenna bandwidth. It is also indicated that once the maximum antenna sizes are given the SISO system with both transmitting and receiving antenna being directional has the potential to achieve the highest information capacity. If both the transmitting antenna and the receiving antenna are small ($ka < 1$), (64)–(67) may reduce to

$$\max C_m|_{d-d}^{small} = \log_2 \left\{ 1 + \frac{p}{\sigma^2} \cdot \frac{\pi}{k^2} \cdot \frac{1}{B_1 B_2} \cdot \frac{6(ka_1)^3}{2(ka_1)^2 + 1} \cdot \frac{6(ka_2)^3}{2(ka_2)^2 + 1} \right\} \quad (69)$$

$$\max C_m \Big|_{o-o}^{small} = \log_2 \left\{ 1 + \frac{p}{\sigma^2} \cdot \frac{\pi}{k^2} \cdot \frac{1}{B_1 B_2} \cdot \frac{3(ka_1)^3}{2(ka_1)^2 + 1} \cdot \frac{3(ka_2)^3}{2(ka_2)^2 + 1} \right\} \quad (70)$$

$$\begin{aligned} \max C_m \Big|_{d-o}^{small} &= \max C_m \Big|_{o-d}^{small} \\ &= \log_2 \left\{ 1 + \frac{p}{\sigma^2} \cdot \frac{\pi}{k^2} \cdot \frac{1}{B_1 B_2} \cdot \frac{6(ka_1)^3}{2(ka_1)^2 + 1} \cdot \frac{3(ka_2)^3}{2(ka_2)^2 + 1} \right\} \end{aligned} \quad (71)$$

respectively. For a high signal-to-noise ratio p/σ^2 , the above equations imply that

$$\max C_m \Big|_{d-d}^{small} \approx 1 + \max C_m \Big|_{d-o}^{small}, \quad \max C_m \Big|_{d-o}^{small} \approx 1 + \max C_m \Big|_{o-o}^{small} \quad (72)$$

Therefore the upper bound of the capacity of a two small directional antenna system is about 2 bit/s/Hz higher than that of a two small omni-directional antenna system.

5.2.2. MISO System

Consider a system consisting of n_t transmitting antennas and one receiving antenna, as shown in Figure 16, where the first n_t antenna are transmitting and the antenna $n_t + 1$ is receiving. In this case (63)

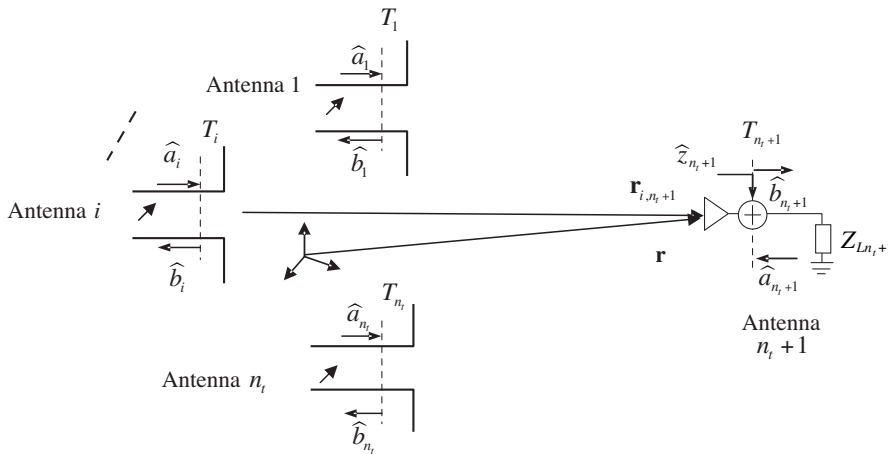


Figure 16. A multiple transmitting antenna system.

reduces to

$$C'_m = \log_2 \left[1 + \frac{P}{4\sigma^2 k^2 n_t} \sum_{i=1}^{n_t} \frac{G_{n_t+1}(-\mathbf{u}_{r_{i,n_t+1}}) G_i(\mathbf{u}_{r_{i,n_t+1}})}{r_{i,n_t+1}^2} \right] \quad (73)$$

If $G_i(\mathbf{u}_{r_{i,n_t+1}})$, $G_{n_t+1}(-\mathbf{u}_{r_{i,n_t+1}})$ and r_{i,n_t+1} can be treated as a constant (i.e., independent of i), (73) reduces to (68). Therefore the capacity of a MISO system in free space does not increase as the number of transmitting antennas increases, which agrees with our usual understanding.

5.2.3. SIMO System

Consider a system consisting of $n_r + 1$ antennas as shown in Figure 17, where antenna $n_r + 1$ is transmitting and the rest antennas are receiving. In this case (62) reduces to

$$C_m = \log_2 \left[1 + \frac{P}{4\sigma^2 k^2} \sum_{i=1}^{n_r} \frac{G_i(-\mathbf{u}_{r_{n_r+1,i}}) G_{n_r+1}(\mathbf{u}_{r_{n_r+1,i}})}{r_{n_r+1,i}^2} \right] \quad (74)$$

Comparing (74) with (73), one immediately finds that the right-hand side of (74) is higher than that of (73) if n_t and n_r are identical.

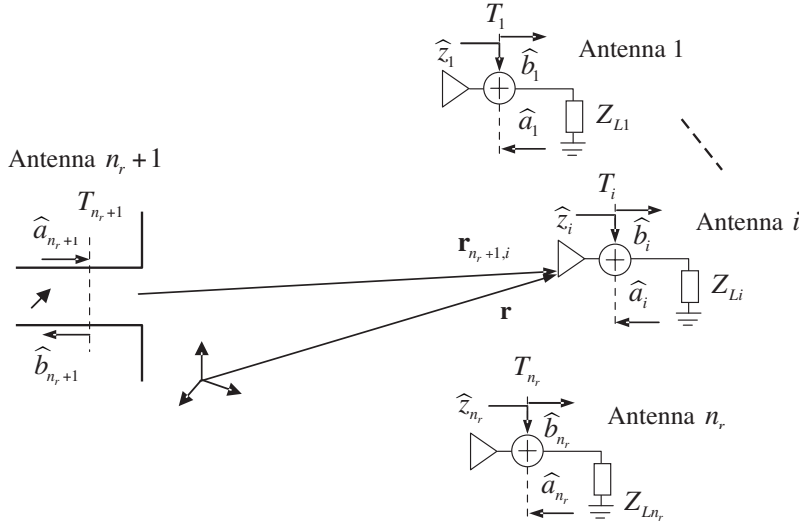


Figure 17. A multiple receiving antenna system.

This implies that the capacity increases with the number of receiving antennas and agrees with our usual understanding about the SIMO system. Assuming that $G_i(-\mathbf{u}_{r_{n_r+1,i}})$, $G_{n_r+1}(\mathbf{u}_{r_{n_r+1,i}})$, and $r_{n_r+1,i}$ can be treated as a constant (i.e., independent of i) so that one may write $G_i(-\mathbf{u}_{r_{n_r+1,i}}) \approx G$ and $G_{n_r+1}(\mathbf{u}_{r_{n_r+1,i}}) \approx G_{n_r+1}$, $r_{n_r+1,i} \approx r$, the right-hand side of (74) can be expressed as

$$C_m = \log_2 \left(1 + \frac{p}{\sigma^2} \frac{\pi}{k^2} n_r G_{n_r+1} G \right) \quad (75)$$

where $p = P/4\pi r^2$. If the capacity and the transmitting antenna gain G_{n_r+1} are specified, (75) can be used to estimate how many receiving antennas are needed to achieve the capacity. For example, if the specified information capacity is C_0 , one may obtain

$$C_0 \leq \log_2 \left(1 + \frac{p}{\sigma^2} \frac{\pi}{k^2} n_r G_{n_r+1} G \right) \approx \log_2 n_r + \log_2 \left(\frac{p}{\sigma^2} \frac{\pi}{k^2} G_{n_r+1} G \right) \quad (76)$$

from (75) for large p/σ^2 . It follows that the number of antenna elements required to achieve C_0 must satisfy

$$n_r \geq 2^{C_0 - \log_2 \left(\frac{p}{\sigma^2} \frac{\pi}{k^2} G_{n_r+1} G \right)} \quad (77)$$

This indicates that the use of high gain antenna can reduce the number of antenna elements required to achieve the specified information capacity C_0 . Also from (76) one may obtain

$$G \geq 2^{C_0 - \log_2 \left(n_r \frac{p}{\sigma^2} \frac{\pi}{k^2} G_{n_r+1} \right)} \quad (78)$$

This inequality combined with (57) can be used to determine the antenna size. For example, if the receiving antennas are omnidirectional and small, one can introduce (59) into (78) to get

$$a \geq \frac{1}{k} \sqrt[3]{\frac{B}{3}} 2^{\frac{1}{3}} \left[C_0 - \log_2 \left(n_r \frac{p}{\sigma^2} \frac{\pi}{k^2} G_{n_r+1} \right) \right] \quad (79)$$

The right-hand side of (79) gives the minimum antenna size required to achieve the capacity C_0 , and also answers the question as to how many independent antennas can be squeezed into a given small volume to satisfy a given capacity requirement, proposed in [20].

6. CONCLUSION

The multiple-input and multiple-output (MIMO) systems have become an increasingly important research area in wireless communication society, and the capacity of MIMO systems has been intensively investigated [e.g., 37–41]. In this paper, an attempt has been made to bridge the gap between information theory and electromagnetic theory, and the MIMO channel capacity has been studied from the electromagnetic point of view. It has been shown that the channel matrix can be identified as the scattering matrix of the multiple antenna system, and the channel matrix elements are related to antenna parameters. Since the antenna parameters have upper bounds once maximum antenna dimensions are specified, the capacity of a wireless MIMO has upper bounds related to the maximum dimension of the antennas. These upper bounds of capacity can be used to estimate the antenna numbers (or real estate) demanded to achieve certain capacity requirement. The procedure of predicting the channel matrix discussed in the paper is applicable to a general MIMO system with a complicated environment, and may be used to determine the site-specific channel models through numerical simulations. In this respect, much more work has yet to be done.

ACKNOWLEDGMENT

The author would like to thank Mr. Dong Wang for his help with experiments.

REFERENCES

1. Shannon, C. E., "A mathematical theory of communication," *Bell Syst. Tech. J.*, Vol. 27, 379–423, July 1948; Vol. 27, 623–656, Oct. 1948.
2. Shannon, C. E., "Communication in the presence of noise," *Proc. IRE*, Vol. 37, 10–21, Jan. 1949.
3. Foschini, G. J. and M. J. Gans, "On limits of wireless communications in a fading environment when using multiple antennas," *Wireless Personal Communications*, Vol. 40, No. 6, 311–335, 1998.
4. Telatar, I. E., "Capacity of multi-antenna Gaussian channels," *Europ. Trans. Telecomm.*, Vol. 10, 585–595, Nov. 1999.
5. Paulraj, A., R. Nabar, and D. Gore, *Introduction to Space-Time Wireless Communications*, Cambridge University Press, 2003.

6. Tse, D. and P. Viswanath, *Fundamentals of Wireless Communications*, Cambridge University Press, 2005.
7. Proakis, J. G., *Digital Communications*, 3rd edition, McGraw-Hill, 1995.
8. Ziemer, R. E. and R. L. Peterson, *Introduction to Digital Communication*, Prentice Hall, 2001.
9. Waldschmidt, C., S. Schulteis, and W. Wiesbeck, "Complete RF system model for analysis of compact MIMO array," *IEEE Trans. Veh. Tech.*, Vol. 53, No. 3, 579–586, May 2004.
10. Wiesbeck, W. and E. Heidrich, "Wide-band multiport antenna characterization by polarimetric RCS measurements," *IEEE Trans. Antennas Propag.*, Vol. 46, No. 3, 341–350, March 1998.
11. Lau, B. K., S. M. S. Ow, G. Kristensson, and A. F. Molisch, "Capacity analysis for compact MIMO systems," *IEEE 61st Veh. Tech. Conference*, 165–170, 2005.
12. Janaswamy, R., "Effect of element mutual coupling on the capacity of fixed linear arrays," *IEEE Antennas Wireless Propag. Lett.*, Vol. 1, 157–160, 2002
13. Gustafsson, M. and S. Nordebo, "On the spectral efficiency of a sphere," *Progress In Electromagnetics Research*, PIER 67, 275–296, 2007.
14. Wallace, J. W. and M. A. Jensen, "Mutual coupling in MIMO wireless systems: A rigorous network theory analysis," *IEEE Trans. Wireless Comm.*, Vol. 3, No. 4, 1317–1325, July 2004.
15. Yu, K. and B. Ottersten, "Models for MIMO propagation channels: a review," *Wirel. Commun. Mob. Comput.*, 653–666, 2002.
16. Sarkar T. K., et al., "A discussion about some of the principles/practices of wireless communication under a Maxwellian framework," *IEEE Trans., Antennas and Propagat.*, Vol. AP-54, 3727–3745, Dec. 2006.
17. Chu, L. J., "Physical limitations of omni-directional antennas," *J. Appl. Phys.*, Vol. 19, 1163–1175, 1948.
18. Harrington, R. F., "Effect of antenna size on gain, bandwidth, and efficiency," *Journal of Research of the National Bureau of Standards-D. Radio Propagation*, Vol. 64D, No. 1, Jan.–Feb. 1960.
19. Geyi, W., "Physical Limitations of Antenna," *IEEE Trans., Antennas and Propagat.*, Vol. AP-51, 2116–2123, 2003.
20. Simon, S. H., A. L. Moustakas, M. Stoytcheve, and H. Safar, "Communication in a disordered world," *Physics Today*, September 2001.

21. Gallager, R. G., *Information Theory and Reliable Communication*, John Wiley & Sons, 1968.
22. Cover, T. M. and J. A. Thomas, *Elements of Information Theory*, John Wiley & Sons, 1991.
23. Jones, D. S., *Elementary Information Theory*, Clarendon Press, 1979.
24. Pinsker, M. S., *Information and Information Stability of Random Process*, Holden Bay, San Francisco, 1964.
25. Marcuvitz, N., *Waveguide Handbook*, McGraw-Hill Book Company Inc., 1951.
26. Vendelin, G. D., A. M. Pavio, U. L. Rohde, *Microwave Circuit Design Using Linear and Nonlinear Techniques*, 2nd edition, Wiley-Interscience, 2005.
27. Gradshteyn, I. S. and I. M. Ryzhik, *Tables of Integrals, Series, and Products*, 6th edition, Academic Press, 2000.
28. Horn, R. A. C. R. Johnson, *Matrix Analysis*, Cambridge University Press, 1985.
29. Harrington, R. F., *Time Harmonic Electromagnetic Fields*, McGraw-Hill, New York, 1961.
30. Balanis, C. A., *Antenna Theory: Analysis and Design*, 2nd edition, John Wiley & Sons, Inc., 1997.
31. Carter, P. S., "Circuit relations in radiating systems and applications to antenna problems," *Proc. IRE*, Vol. 20, No. 6, 1004–1041, June 1932.
32. Schelkunoff, S. A., *Antennas: Theory and Practice*, John Wiley & Sons, Inc., 1952.
33. Monteath, G. D., *Applications of the Electromagnetic Reciprocity Principle*, Pergamon Press, 1973.
34. Popvić, B. D., "Electromagnetic field theorems," *IEE Proc. on Science Measurement and Technology*, Vol. 128, Pt. A, 47–63, Jan. 1981.
35. Fante, R. L., "Quality factor of general idea antennas," *IEEE Trans. Antennas and Propagat.*, Vol. AP-17, 151–155, 1969.
36. Geyi, W., P. Jarmuszewski, and Y. Qi, "Foster reactance theorems for antennas and radiation Q," *IEEE Trans. Antennas and Propagat.*, Vol. AP-48, 401–408, Mar. 2000.
37. Geyi, W., "New magnetic field integral equation for antenna system," *Progress In Electromagnetic Research*, PIER 63, 153–170, 2006.

38. Chen, Y. B., Y. C. Jiao, F. S. Zhang, and H. W. Gao, "A novel small CPW-fed T-shaped antenna for MIMO system applications," *J. of Electromagn. Waves and Appl.*, Vol. 20, No. 14, 2027–2036, 2006.
39. Abouda, A. A., H. M. El-Sallabi, and S. G. Häggman, "Effect of antenna array geometry and ULA azimuthal orientation on MIMO channel properties in urban city street grid," *Progress In Electromagnetics Research*, PIER 64, 257–278, 2006.
40. Abouda, A. A., and S. G. Häggman, "Effect of mutual coupling on capacity of MIMO wireless channels in high SNR scenario," *Progress In Electromagnetics Research*, PIER 65, 27–40, 2006.
41. Li, H.-J. and C.-H. Yu, "MIMO channel capacity for various polarization combinations," *J. of Electromagn. Waves and Appl.*, Vol. 18, No. 3, 301–320, 2004.